

# Quantitative physicochemical analysis of equilibria on chemically modified silica surfaces\*

Yuriy Kholin<sup>1,‡</sup> and Vladimir Zaitsev<sup>2</sup>

<sup>1</sup>V. Karazin Kharkiv National University, 4 Svoboda Square, Kharkiv, 61077, Ukraine; <sup>2</sup>Kiev National Taras Shevchenko University, 60 Volodymyrska Str., Kiev, Ukraine

**Abstract:** Quantitative physicochemical analysis (QPCA) enables the determination of the stoichiometric compositions and physicochemical parameters of species in equilibrium systems proceeding from the composition–property dependencies. The paper discusses modifications to the routine QPCA procedures required to characterize properties of reagents fixed on surfaces of silica–organic hybrid materials. The cooperative effects and the energetic heterogeneity of fixed reagents are especially important in this context. It follows that the main peculiarities of silica surfaces chemically modified by aliphatic amines are (a) the pronounced energetic heterogeneity of reagents caused by the non-random surface topography, (b) the decrease of the basicity of amines induced by their interactions with residual surface silanols, and (c) the expressed sensibility of reactions in the near-surface layer to the state of its hydration. The interaction of grafted organic bases with metal ions results in the preferred formation of *bis* metal-ligand coordination compounds. Stability constants of complexes are decreased as a consequence of fixation and depend on not only donor but also acceptor ability of a solvent. Also, the denticity of polydentate ligands may decrease as a result of grafting. The changes of protolytic and complexing properties in the case of grafting of weak acids and phosphorus-containing complexons are due to their interactions with other surface groups and the influence of hydration effects in the near-surface layer.

**Keywords:** quantitative physicochemical analysis; chemically modified surfaces; cooperativity effects; surface energetic heterogeneity; silica–organic hybrid materials; grafted reagents; chemisorption; protolytic and complexing properties; simulation of surface equilibria.

## INTRODUCTION

Hybrid materials prepared by combining silica with various organic species have been attracting growing attention during the last three decades (see, e.g., [1–12]). Resulting materials retain mechanical properties and the main morphological features of inorganic support that provides favorable kinetic characteristics of sorption or ion-exchange processes [9,11,13]. The present-day synthetic procedures enable the introduction of practically all desired organic reagents into hybrid materials, making it possible to regulate the affinity of materials to target species [5,11–17]. Significant progress of the sol-gel procedures during the last 15 years [18–21] resulted in even greater diversity of hybrid materials and

\*Paper based on a presentation at the International Conference on Modern Physical Chemistry for Advanced Materials (MPC '07), 26–30 June 2007, Kharkiv, Ukraine. Other presentations are published in this issue, pp. 1365–1630.

‡Corresponding author. Tel.: +380 57 707 51 43; E-mail: kholin@univer.kharkov.ua

areas of their application. Now, hybrid silica–organic materials are proven to be efficiently used as selective sorbents and ion exchangers, catalyst supports, stationary phases in chromatography, substrates for immobilization of electroactive species, enzymes, and other biomolecules [22–41].

Generally, there are three main ways to create hybrid silica–organic materials. Cheap and fast noncovalent immobilization of organic reagents (predominantly, acid–base and compleximetric indicators) on amorphous silica surfaces is used widely to obtain solid-phase reagents for visual or spectroscopic detection and determination of metal ions [42–44]. As the noncovalent retention is rather weak, such materials lose organic modifiers quickly. The second method includes the silanization of silica surfaces by appropriate silica–organic modifiers [5,9,11,45–47]. The silanization leads to the formation of hydrolytically stable Si–C bonds. Also, the subsequent chemical modification of the attached groups is performed. The third way is the one-pot sol-gel synthesis of functionalized silicas [48–51].

Irrespective of the preparation routine, the properties of silica–organic hybrids are not the sum of the properties of unmodified inorganic support and native organic modifiers. The behavior of a material can be affected by the chemical activity of a silica surface and the interaction of surface silanols with modifiers, unusual properties of a solvent in the near-surface layer, the energetic heterogeneity of immobilized reagents, and many other factors. In this context, the principal question arises: How does the immobilization of organic modifiers change their properties or, more definitely, how does the immobilization affect the affinity of attached reagents to “ligands”<sup>\*</sup>? The answer to this question is important from two points of view. First, the comprehensive information about features of immobilized reagents is necessary to choose the optimal conditions for sorption or ion-exchange concentration, extraction, separation, and removal of ligands from solutions, etc. Second, this information allows us to understand better the properties of hybrid materials and to forecast and regulate their affinity to ligands at the stage of synthesis. Among many methods applied to study the hybrid materials, quantitative physicochemical analysis (QPCA) is of special significance. QPCA is the only approach that allows us to determine not only the stoichiometry of the ligand–reagent interactions, but also the thermodynamic characteristics of these processes. QPCA has a long history; nevertheless, its expansion into the new field significantly touches its methodological foundations. The meaningful models will be discussed in this connection as the main tool to handle the primary experimental data within QPCA. The calculation procedures, a separate important aspect of QPCA, exceed the bounds of this paper and are touched only occasionally. Also, the results obtained within QPCA for different classes of chemically modified silicas will be reported. These data provide new important information about the influence of different factors on the ligand-attached reagent interactions and allow us to find correlations useful for forecasting the composition and stability of surface complexes.

## FOUNDATIONS OF QUANTITATIVE PHYSICOCHEMICAL ANALYSIS

According to Nikolai Kurnakov, one of the pioneers of physicochemical analysis, the very first work in this field was performed in the 3<sup>rd</sup> century BC by Archimedes when he measured the density of the Au–Ag system to check the authenticity of King Hieron’s gold crown [52]. The foundations of modern physicochemical analysis were laid by Dmitry Mendeleev who detected the so-called “hydrates of ethanol” and found their stoichiometric compositions from the dependence of densities of ethanol–water mixtures on the weight percentage of ethanol [53]. During the last century, physicochemical analysis was essentially developed and transformed into QPCA. Now, QPCA is an assemblage of experimental methods and computational tools for the determination of stoichiometric composition and various physicochemical characteristics of species in equilibrium systems by registering and analyzing the composition–property dependencies [54]. QPCA grants the indispensable information. For

<sup>\*</sup>Any ion or small molecule which associates with attached reagents is termed “ligand”, and products are termed “complexes”.

instance, the comprehensive information about the stability constants of metal ion complexes in solutions was obtained [55]. These data enable the construction of many correlations useful for predicting stability constants, and the generalization of the obtained results facilitated better understanding of the principal questions of coordination chemistry and was important from a practical point of view [56–60].

Consider briefly the main peculiarities of QPCA when applied to studying equilibria on surfaces of hybrid materials. Let a dissolved ligand M interact with functional groups Q of the material with the formation of one or several bound complexes (we shall denote them  $M_mQ_q$ , where  $m$  and  $q$  are the stoichiometric indices). The primary experimental data can be presented as a composition–property dependence:

$$g_k = \varphi[t_k(M), t_k(Q), t_k(X), \dots, a_k, V_k] \quad (1)$$

where  $g$  is the measured property (amount of M remaining in solution at equilibrium, pH of solution, etc.);  $X$  are the reagents present in solution (except for M);  $t(Q)$  is the effective specific concentration of groups Q;  $t(M)$ ,  $t(X)$  are the total (initial) concentrations of reagents in solution known from the conditions of preparations;  $a$  is the weight of a material;  $V$  is the initial volume of a liquid phase;  $k$  is the number of experimental point; and  $\varphi$  is a certain (a priori unknown) function. When the surface complexation is studied, adsorption of M ( $N_f$ ) is often used as the measured property of the equilibrium system. Usually, it is determined as

$$N_f = V \times \frac{t(M) - [M]}{a} \quad (2)$$

where  $[M]$  is the equilibrium concentration of M in solution.

The aim of QPCA is to determine, on the basis of dependence 1, the number of complexes fixed on the surface and their stoichiometric composition and thermodynamic stability.

QPCA consists of three main interrelated steps: structural identification of the model, parametric identification of the model, and estimation of the model adequacy [61]. Also, it is desirable to verify the model with the use of independent data.

## STRUCTURAL IDENTIFICATION OF MODELS

Whatever the structure of a model, it must contain equations of three types: (a) equations describing the relationships between the measured property  $g$  and the equilibrium composition of the system; (b) the material balance equations; and (c) equations of the mass action law or their analogs. The construction of equations of first two groups is evident, but it is essentially more complicated for the third group. On the one hand, the peculiar properties of bound species need to be taken into account explicitly. On the other hand, any chosen form of the model must agree with the general principles of thermodynamics. In spite of the long-term efforts, the thermodynamic description of processes at the amorphous solid–liquid interfaces remains the “hot” subject that is evident from the ceaseless discussions in the literature (see, e.g., [62–66]). However, some important aspects have been clarified well enough. Complex formation takes place at the solution–solid interface. Hence, one of the thermodynamic languages, the Gibbs method or the finite-thickness layer method [67,68], is relevant in describing this process. It is also important to take into account that the true thermodynamic components of any system (substances which can be introduced into it independently) are a solvent, ligands M and supermolecules [69] of the material. Any supermolecule contains a certain amount of support  $\text{SiO}_2$  and several organic groups Q, and its general formula can be written as  $\{\text{SiO}_2\}_xQ_y\}$ , where  $x$  and  $y$  are the stoichiometric indices. Considering supermolecule  $\{\text{SiO}_2\}_xQ_y\}$  as a single  $y$ -dentate binding center, one can describe the sorption of M as the stepwise addition of ligands M to  $\{\text{SiO}_2\}_xQ_y\}$  with the formation of products  $\{\text{SiO}_2\}_xQ_yM\}$ ,  $\{\text{SiO}_2\}_xQ_yM_2\}$ , ...,  $\{\text{SiO}_2\}_xQ_yM_n\}$ , ...,  $\{\text{SiO}_2\}_xQ_yM_y\}$ . The process is characterized by a set of equilibrium constants  $\gamma_n$ :

$$\gamma_n = \{(\text{SiO}_2)_x \text{Q}_y \text{M}_n\} / \{(\text{SiO}_2)_x \text{Q}_y\} \cdot [\text{M}]^n \quad (3)$$

where  $n$  is the number of ligands M attached to the supermolecule.

In the rigorous Gibbs method, the adsorption is an excessive quantity, and surface or specific concentrations of fixed groups Q and complexes lose their meaning. As a result, not only the calculation of stability constants of bound complexes but even the determination of their stoichiometric compositions become meaningless. In terms of the less strict finite-thickness layer method [61,68], the system is considered as consisting of three phases: an inner volume of a solid with properties not affected by interactions of ligands M with groups Q; a homogeneous liquid phase; and a heterogeneous adsorption layer (AL)\*. By definition, adsorption ( $X$ ) is assumed to be the total amount of M in the adsorption layer:

$$X = \frac{1}{a} \int_{z_1}^{z_2} c(z) dz \quad (4)$$

where  $c(z)$  is the concentration of M in AL varying along the normal ( $z$ ) to the surface;  $z_1$  and  $z_2$  are positions of inner and outer boundaries of AL, respectively.  $X$  depends on the choice of  $z_2$ : it increases with the increase of  $z_2$ . The difference between  $X$  and  $N_f$  reads

$$N_f - X = \frac{(V^{\text{eq}} - V)[\text{M}]}{a} \quad (5)$$

where  $V^{\text{eq}}$  is the equilibrium volume of solution minus the volume included in AL. As hybrid materials do not swell practically in solutions, and volumes of diluted solutions are changed slightly during reactions, the difference between  $N_f$  and  $X$  is considered as negligible. This allows us to equate  $N_f$  to  $X$ , bearing in mind, however, the somewhat approximate character of this approach. The necessity to introduce further simplifying approximations follows from the lack of information about the distribution of reagents in AL. To introduce expressions for their equilibrium concentrations, one has to “tighten” the adsorption layer. In the limiting case, AL is compressed to the monolayer, and boundaries  $z_1$  and  $z_2$  are drawn in such a way that the thickness of AL is equal to the diameter of a ligand. Then the problem of the AL heterogeneity disappears, and the surface or specific concentrations of bound groups and complexes may be used instead of the undetermined concentrations of reagents in AL\*\*. Unfortunately, under this simplification, the initial assumptions about the properties of the inner volume of a solid and the solution phase are disturbed, which complicates the interpretation of the simulation results.

The binding of ligands M with surface-active centers Q can be treated as a special case of association of ligands with a multisite lattice. The interaction of ligands M and centers Q with the formation of surface complexes  $\overline{\text{MQ}}$



is of the ideal character if complexes of only one type are formed, all centers Q are energetically homogeneous, and lateral interactions are negligible. In this case, the structure of the model is specified by the Langmuir equation [71]:

$$[\overline{\text{MQ}}] = t(Q) \times \frac{\beta[\text{M}]}{1 + \beta[\text{M}]} \quad (7)$$

\*AL is not the true macroscopic phase and belongs to the family of pseudophases, well known in physical chemistry of organized solutions.

\*\*In this context, the success of the early practice (see, e.g., [4,70]), when the concentrations of bound species were related to the solution volume, looks rather strange.

Here,  $[\overline{MQ}]$  is the specific equilibrium concentration of the bound ligand, and  $\beta$  is the heterogeneous stability constant of complex  $\overline{MQ}$ . More complicated models are necessary to take into account the non-ideality effects. The great diversity of models describing the non-ideality was developed separately in different scientific areas. This hampers significantly the generalization of the available arrays of data representing the composition and stability of fixed complexes. In this connection, considerable efforts were made to unify the system of models and to find relationships between parameters of different models [61,72–75]. Besides, the scope and reliability of meaningful information extracted with the help of these models from the primary experimental data were studied. Now it is possible to state that the majority of models describing the non-ideal sorption at surfaces of hybrid silica–organic materials can be combined into a unified system, and models of two types are recommended for the practical use.

Models of the first type detect and describe the effects of biographic energetic heterogeneity [71,76–80], while models of the second type characterize the cooperativity effects [80–83]. The biographic heterogeneity of surfaces is considered as the intrinsic feature of the material [84]. It is postulated that there exists a distribution of binding sites  $Q$  in the affinity constants  $\beta$ ,  $p(\beta)$ , and the degree of occupation of sites does not affect the affinity of each site to  $M$ . The biographic heterogeneity may be due to the heterogeneous surface topography, the presence of pores of different shape and size, the chemical heterogeneity of binding centers, and other reasons [79].

The cooperativity effects are often considered in polymer chemistry, biochemistry, ion adsorption from solutions, etc. It is assumed that all binding centers  $Q$  have the same intrinsic affinity to ligands, and “where cooperativity takes place the affinity of the ligand for the receptor site may be enhanced (positive cooperativity) or depressed (negative cooperativity) by previous occupation of sites” [83]. There are many possible molecular mechanisms of the cooperativity, for instance, the site–site interactions or the electrostatic repulsion of a charged ligand from a charged surface.

## DESCRIPTION OF BIOGRAPHIC ENERGETIC HETEROGENEITY

Discussion of the biographic energetic heterogeneity is restricted here to the monocomponent binding. The quantitative description of the effects of energetic heterogeneity includes the following steps: (1) measurement of the dependence of  $f$  on  $[M]$  where  $0 \leq f([M]) \leq 1$  is a fraction of binding centers  $\overline{Q}$  occupied with  $M$ , square brackets denote equilibrium concentrations of species in solution; (2) postulation of a model which allows us to separate the effects of biographic heterogeneity and cooperativity; and (3) calculation numerically of the model parameters. To perform step 3, it is necessary to solve one of the following equations [71]:

$$f([M])_k = \int_0^{\infty} \theta^{\text{local}}([M]_k, \beta) \cdot p(\beta) d\beta, \quad k = 1, 2, \dots, N \quad (8)$$

or

$$f([M])_k = \sum_{j=1}^J \theta^{\text{local}}([M]_k, \beta_j) \cdot p(\beta_j), \quad k = 1, 2, \dots, N \quad (9)$$

where  $N$  is the number of experimental points,  $J$  is the number of knots within the interval of variation of  $\beta$ ,  $\beta_j$  is the value of  $\beta$  at the  $j$ -th knot with respect to  $p(\beta)$ ,  $p(\beta)$  being the non-negative density function of constants  $\beta$  (continuous or discrete, depending on the choice of equation to be solved); the kernel of the integral equation  $\theta^{\text{local}}([M], \beta)$  is the local binding isotherm. The density function  $p(\beta)$  describes the biographic heterogeneity, while the effects of cooperativity are taken into consideration by choosing an appropriate expression for the local isotherm. In addition to  $p(\beta)$ , the integral distribution function

$$P(\beta) = \int_0^{\beta} p(x)dx, \quad 0 \leq P(\beta) \leq 1 \quad (10)$$

can be used to characterize the biographic energetic heterogeneity.

It should be particularly emphasized that the deviation from the ideal binding can be equally well described in terms of the biographic heterogeneity or the cooperativity effects. Accordingly, it can be attributed to the simultaneous action of both of them [79,80]. Thus, there are no decisive experimental data to prefer one or another function for a local isotherm. In the limiting case when both electrostatic and lateral interactions are negligible, the kernel  $\theta^{\text{local}}([M], \beta)$  reduces to the Langmuir isotherm

$$\theta^{\text{local}}([M], \beta) = \frac{\beta \cdot [M]}{1 + \beta \cdot [M]} \quad (11)$$

Sometimes this choice can be validated *a posteriori*. For this, the binding isotherms are measured at different ionic strengths of solution ( $I$ ), and the corresponding density functions  $p(\beta)$  are calculated. If the shapes of functions  $p(\beta)$  and positions of their maxima do not depend significantly on  $I$ , it may be concluded that the choice of the Langmuir isotherm was justified [85].

It is possible to demonstrate the way in which functions  $p(\beta)$  and  $P(\beta)$  are connected with constants  $\gamma_n$  that describe hybrid material  $\{\text{SiO}_2\}_x \text{Q}_y\}$  as a single binding center. It is well known that a  $y$ -acid base,  $B$ , demonstrates the same pH-titration curve as an equimolar mixture of  $y$  hypothetical monoacid bases, the protonization constants of these monoacid bases ( $\beta_i$ ) being unambiguously connected with the overall protonization constants ( $\gamma_n$ ) of a polyacid base [86]:

$$\gamma_n = \sum_{v_i \in \Xi} \beta_1^{v_1} \times \beta_2^{v_2} \times \beta_i^{v_i} \times \dots \times \beta_y^{v_y}, \quad n = 1, 2, \dots, y \quad (12)$$

where the set  $\Xi$  is defined by the following conditions:

$$v_i \leq 1; \quad v_i \geq 0; \quad \sum_{i=1}^y v_i = n, \quad i = 1, 2, \dots, y \quad (13)$$

For example, if  $y = 3$ , then

$$\gamma_1 = \beta_1 + \beta_2 + \beta_3, \quad \gamma_2 = \beta_1 \cdot \beta_2 + \beta_1 \cdot \beta_3 + \beta_2 \cdot \beta_3, \quad \gamma_3 = \beta_1 \cdot \beta_2 \cdot \beta_3 \quad (14)$$

It was shown that the pH-dependence of *any* property of a polyacid base (polybasic acid) may be represented by the sum of one-site titration curves [87,88]. On the other hand, it is possible to approximate the distribution function  $P(\beta)$  by the  $y$ -step one (Fig. 1). At high  $y$ , the error of approximation is negligibly small. So, if a binding isotherm is described in terms of an affinity statistical distribution of  $y$ -independent sites, this isotherm may be equally well described in terms of  $y$ -step addition of ligands to the  $y$ -dentate center, and vice versa.

From the mathematical standpoint, eq. 8 is the first-kind Fredholm integral equation, and the calculation of density function  $p(\beta)$  and/or distribution function  $P(\beta)$  from the primary experimental data is a typical example of ill-posed problems. It means that many different possible solutions  $p(\beta)$  fitting the measured  $f([M])$  dependence within the experimental errors may exist. Moreover, small fluctuations in primary experimental data  $\{[M]\}$  or  $f([M])\}$  may cause arbitrary large fluctuations in the calculated density function  $p(\beta)$ . A lot of calculation procedures, predominantly based on Tikhonov's  $\alpha$ -regularization approach [89], were developed to solve the problem. The comparison of modern calculation approaches can be found elsewhere [90,91]. The commonly used procedures require implicit or explicit assumptions about the smoothness of the searched density function  $p(\beta)$  and/or the distribution law of the experimental errors in  $f([M])$ . Some imminent properties of these procedures are especially unfa-

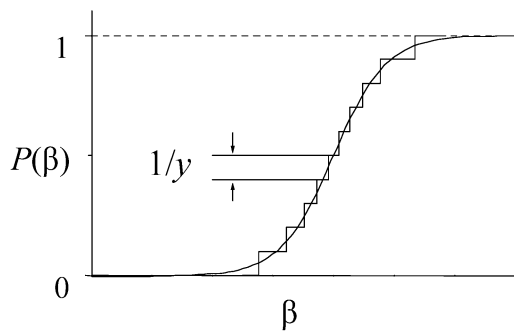


**Fig. 1** Approximation of the distribution function  $P(\beta)$  by the  $y$ -step one.

vorable in the case of narrow density functions  $p(\beta)$ . To overcome this drawback, a new approach based on the maximum entropy method was recently proposed [91,92]. The discrete density function  $p(K)$  is obtained through maximizing the Shannon entropy [93]

$$S = - \sum_{j=1}^J p(\beta_j)_j \times \log p(\beta_j)_j \quad (15)$$

subjected to known constraints

$$\sum_{j=1}^J p(\beta_j) \times \frac{\beta_j \cdot [M]_k}{1 + \beta_j \cdot [M]_k} \geq f_k^{\text{measured}} - \Delta, \quad k = 1, 2, \dots, N \quad (16)$$

$$\sum_{j=1}^J p(\beta_j) \times \frac{\beta_j \cdot [M]_k}{1 + \beta_j \cdot [M]_k} \leq f_k^{\text{measured}} + \Delta, \quad k = 1, 2, \dots, N \quad (17)$$

$$\sum_{j=1}^J p(\beta_j) = 1, \quad p(\beta_j) \geq 0 \quad (18)$$

where  $J$  is the number of knots, and threshold  $\Delta$  is the highest supposed value of experimental error in  $f([M])$ . The minimum possible value of  $\Delta$  ( $\Delta_{\min}$ ) is such a value that provides the compatibility of the system. The method does not require any additional information about the experimental errors. If such information is available, it may be taken into consideration easily by the appropriate modification of inequalities 16 and 17. Numerical simulations have shown that the proposed algorithm works well even in the case of very close and narrow density functions  $p(\beta)$  [91].

## MODELS OF FIXED POLYDENTATE CENTERS AND CHEMICAL REACTIONS

The main models used to find the stoichiometric composition and equilibrium constants of the surface complexation reactions are the models of fixed polydentate centers and chemical reactions [61,70,72,73,94–98]. Both are special cases of the general lattice model. It is postulated that (a) the monolayer adsorption takes place, (b) the values of stability constants of fixed complexes depend only on their stoichiometric composition and are independent of the occupation degrees of binding centers, and (c) binding of charged ligands is accompanied by the counterion penetration into the near-surface layer that provides the electroneutrality of solution, support, and adsorption layer.

The model of fixed polydentate centers was independently reinvented several times in different branches of chemistry [94,97,99]. The reactive surface is considered as an assemblage of polydentate

binding centers  $\overline{Q}_Z$ , each center being composed of  $Z$  groups  $Q$ . The specific concentration of centers  $\overline{Q}_Z$  is equal to  $t(Q)/Z$ . The binding of ligands by centers  $\overline{Q}_Z$  is treated as the stepwise process that is characterized by  $Z$  values of equilibrium constants  $\sigma_i^{(Z)}$  (where  $i$  is the step number). Figure 2 illustrates how the model of bidentate centers ( $Z = 2$ ) treats the protonization of fixed amines. The model is extended in an evident way to the description of the competitive multicomponent binding.

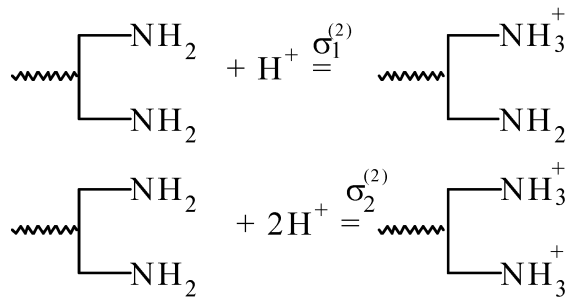


**Fig. 2** Protonization of the grafted amino groups in the model of fixed bidentate centers.

The construction of the model starts from the lowest  $Z$  value [98]. The corresponding  $\sigma_i^{(Z)}$  values are calculated through the minimization of an appropriate fitting criterion, and the statistical adequacy of the model is tested. If the model with few fitting parameters does not reproduce the primary composition–property dependence within the limits of experimental errors,  $Z$  is increased and the values of  $\sigma_i^{(Z)}$  are calculated again. The procedure is repeated until the required fitting is achieved. This strategy prevents the construction of redundant models with surplus complexes (which describe an experimental noise rather than extract the meaningful information from the data). Constants  $\sigma_i^{(Z)}$  obtained within the model can be referred to constants  $\gamma_n$  describing a supermolecule as one binding center. The necessary expressions can be found elsewhere [61,74,75].

Information about cooperativity is easily obtained from the results of simulations. When there is no cooperativity, addition of ligands to each active group  $Q$  is characterized by the only intrinsic equilibrium constant. In this case, the ratios of stepwise equilibrium constants\*  $K_{i+1}^{(Z)}/K_i^{(Z)}$  are equal to statistical factors  $(Z - i + 1) \cdot (i + 1) / [i \cdot (Z - 1)]$  [100]. In the case of positive cooperativity, these ratios exceed the statistical factors, while negative cooperativity decreases them. If there is no cooperativity or it is negative, the system of inequalities

$$K_i^{(Z)} < K_{i-1}^{(Z)} < \dots < K_1^{(Z)} \quad (19)$$

is held. The deviation of experimental binding constants from inequalities 19 points to the positive cooperativity.

The model of chemical reactions differs from the model of fixed polydentate centers in that it takes into account not only the protonization of binding centers and the stepwise complex formation, but also another reactions, such as formation of polynuclear or mixed complexes. If the surface reaction



takes place, its equilibrium constant is specified as

---

\*The stepwise equilibrium constants and the overall ones are connected by the conventional relationship:  $\sigma_i^{(Z)} = \prod_{i=1}^Z K_i^{(Z)}$ .

$$\beta_{qm} = \frac{[\overline{M_m Q_q}]}{[M]^m \cdot [\overline{Q}]^q} \quad (21)$$

This equation contains the surface (or specific) concentration of centers Q raised to the  $q$ -th power that looks somewhat strange and casts doubt on the agreement between two models. But in terms of the general lattice model, the model of chemical reactions was shown to be compatible with the model of fixed polydentate centers in the sense that there is the univocal correspondence between the parameters of these models [72]. For example, if the model of chemical reactions taking into account the formation of complexes MQ and  $MQ_2$  is valid, equilibrium constants in the model of Z-dentate centers are given by the following expressions:

$$\sigma_j^{(Z)} = \sum_{v \in \Xi} \frac{G!}{v_1! v_2! v_3!} \times 2^{v_2} \beta_{11}^{v_1} \beta_{21}^{v_2} t(Q)^{v_2}, \quad 0 < j \leq Z \quad (22)$$

where set  $\Xi$  is specified by conditions:  $v_1 \geq 0, v_2 \geq 0, v_3 \geq 0; G = v_1 + v_2 + v_3; j = v_1 + v_2, v_1 + 2 \cdot v_2 + v_3 = Z$ . If  $Z = 2$  (model of bidentate centers), then

$$\sigma_1^{(2)} = 2\beta_{11} + 2\beta_{21} \cdot t(Q), \quad \sigma_2^{(2)} = \beta_{11}^2 \quad (23)$$

The construction of the model of chemical reactions resembles the “top-down” strategy used in the case of the model of fixed polydentate centers. It starts from the simple trial of a hypothesis about reactions. The number of species  $S$  and their stoichiometric compositions are specified, and the unknown equilibrium constants  $\beta = |\beta_j|, j = 1, 2, \dots, Z$ , where  $Z$  is the number of fitting parameters, are calculated through the minimization of a fitting functional [61,101]:

$$M(\boldsymbol{\beta}) = \sum_{k=1}^N \rho(\xi_k^2) \quad (24)$$

Here,  $\rho$  is a certain “loss function” specifying the metrics, weighed discrepancy  $\xi = \Delta_k \cdot w_k^{1/2}$ ,  $\Delta_k = g_k^{\text{calculated}} - g_k^{\text{measured}}$ ,  $w_k$  is the statistical weight assigned according to the model of experimental errors. For example, if the adsorption  $N_f$  was chosen as the measured property, it is possible to assign weights as

$$w_k = \frac{1}{(N_f)^2 s_r^2} \quad (25)$$

where  $s_r$  is the relative standard deviation of  $N_f^{\text{measured}}$  (typically 0.10 or 0.05) [102].

The choice of the loss function  $\rho$  depends on the distribution of experimental errors. If they obey the Gaussian law with zero mean, the maximum likelihood principle justifies the error-squared form of loss function. Then criterion 24 turns into a specific form of the least-squares (LS) method [103]:

$$M(\boldsymbol{\beta}) = \chi_{\text{exp}}^2 = \sum_{k=1}^N \xi_k^2 \quad (26)$$

and estimations  $\boldsymbol{\beta}^*$  corresponding to its minimum are asymptotically unbiased, consistent, and efficient. To avoid the loss of these optimal statistical properties in the case of other distributions of experimental errors, the application of the robust estimations instead of the LS ones was proposed. Huber's quasi maximum-likelihood  $M$ -estimates are considered as a good choice [103–105]. In this case, the loss function becomes a hybrid of metrics inherent to the LS and least-modules methods:

$$\rho(\xi) = \begin{cases} (1/2)\xi^2 & \text{at } |\xi| \leq c_{out} \\ c_{out} \cdot |\xi| - (1/2)c_{out}^2 & \text{at } |\xi| > c_{out} \end{cases} \quad (27)$$

where  $0 \leq \delta \leq 1$  is the fraction of errors obeying the distribution law with tails longer than Gaussian tails; constant  $c_{out}$  depends on  $\delta$  [105]. The calculation procedures and software programs for finding robust estimations of parameters in the QPCA tasks were developed [61,106]. Simultaneously with the  $\beta^*$  values, their dispersion-covariance matrix  $D(\beta^*)$  is calculated that allows us to determine the approximate confidence region of the  $\beta^*$  set together with partial, multiple, and total correlation coefficients of parameters. For testing the adequacy of the model, the global  $\chi^2$  criterion is usually applied [107]. The model is accepted as adequate if inequality

$$\chi_{\exp}^2 < \chi_u^2(5\%) \quad (28)$$

is held, where  $\chi_u^2$  is the 5-percentage point of the chi-square distribution with  $u$  degrees of freedom. If  $\beta^*$  are the LS estimates,  $u = N - Z$ . In the case of Huber's M-estimates

$$u = (N - Z) \times \frac{1}{1 + 0.5\gamma_2(N - Z)/N} \quad (29)$$

where  $\gamma_2$  is the sample excess of weighed discrepancies  $\xi_k$  [105]. If inequality 28 is not fulfilled, it is necessary to introduce additional species into the model and to repeat the calculations. This is required even if the global criterion  $\chi^2$  confirms the adequacy of the model, but discrepancies  $\xi_k$  demonstrate the systematic character. To ascertain better the validity of the model, the conventional statistical procedures are recommended to be supplemented with the cross-validation procedures [108].

The stoichiometric composition of species to be included into the model is chosen by the classical "trial-and-error" approach by applying a suitable species selector [109] or from the analysis of the region of the experiment design with the bad fit [102].

As any problem of parametrical identification, the calculation of  $\beta^*$  is the ill-posed problem. In this specific case, the ill-posed nature of the problem manifests itself in the possibility of redundant species to appear in the model. These species represent the experimental noise rather than the real composition–property dependence, and their stability constants have no meaning. Modern software programs include tools for the elimination of the redundant species based on the inspection of the Jacoby matrix  $J = \|\partial g_k / \partial \log \beta_i\|$  by means of singular-value decomposition [110] or other tools of principal component analysis [59,61,111].

Thus, models of fixed polydentate centers and chemical reactions implemented in modern software programs provide the comprehensive description of complicated systems with the account of cooperativity and formation of bound complexes with peculiar composition and/or stability.

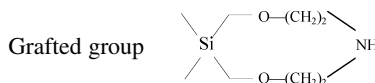
## PROTOLYTIC AND COMPLEXING PROPERTIES OF SILICAS MODIFIED BY ORGANIC BASES

Nowadays, the most widely used and well-studied class of surface-modified silicas is the class of amine-functionalized silicas [5,7,11,46,112]. Many of them are available commercially.

We have studied protolytic properties of primary and secondary amines grafted on silica surfaces [61,90,113–122]. Aminosilica samples were prepared according to the routine procedures [4,45,46,113]. They differ in supports (nonporous aerosils, macroporous silochromes, and porous silica gels), the surface area, and the concentration of grafted groups. One sample of silica with attached *n*-propylamine was prepared according to the specially developed procedure [122], which provides the uniform surface topography. Protolytic properties of aminosilicas were characterized on the base of the

pH-titrations of suspensions of samples in aqueous solutions of 1-1, 1-2, and 2-2 electrolytes over the temperature range 293–323 K. For several samples, supplementary measurements were performed. After the first pH determination, the closed jars with suspensions were allowed to stand at 40 °C for 2 days, then cooled to 20 °C, and the pH was measured again. Additional “heating–cooling” cycles did not change the pH. Characteristics of some studied aminosilicas are presented in Table 1.

**Table 1** Characteristics of aminosilicas.

No	Support	Surface area, m <sup>2</sup> g <sup>-1</sup>	Pore size, nm	Concentration of grafted groups mmol g <sup>-1</sup>	μmol m <sup>-2</sup>
		Grafted group –CH <sub>2</sub> –CH <sub>2</sub> –CH <sub>2</sub> –NH <sub>2</sub>			
1		135		0.024	0.18
2		135		0.14	1.04
3		135		0.16	1.19
4 <sup>a</sup>	Aerosil	175	Nonporous	0.27	1.54
5		175		0.32	1.83
6		115		0.36	3.13
7		175		0.43	2.45
8		130		0.56	4.31
9		300	5–10	0.68	2.23
10	Silica gel	300	5–10	0.78	2.60
11		300	5–10	0.70	2.33
12	Silochrome	120	30–50	0.26	2.17
13 <sup>a</sup>	Aerosil	175	Nonporous	0.43	2.46
14 <sup>b</sup>	Aerosil	200	Nonporous	0.20	1.00
		Grafted group –CH <sub>2</sub> –CH <sub>2</sub> –CH <sub>2</sub> –NH–CH <sub>2</sub> –CH <sub>2</sub> CN			
15	Aerosil	200	Nonporous	0.27	1.35
16	Fractosil	120	20	0.21	1.75
		Grafted group 			
17	Silochrome	120	30–50	0.46	3.83
		Grafted group –CH <sub>2</sub> –CH <sub>2</sub> –CH <sub>2</sub> –NH–CH <sub>3</sub>			
18	Aerosil	200	Nonporous	0.53	2.65
19	Fractosil	120	20	0.35	2.92

<sup>a</sup>Aminosilicas treated with trimethylsilylimidazole (sample 4) or hexamethyldisilazane (sample 13).

<sup>b</sup>Sample with the uniform surface distribution of grafted amines.

For the sample with the uniform surface topography and for the samples exposed to the heating–cooling cycle, the H<sup>+</sup> binding isotherms are described well by Langmuir-type equation

$$\overline{[\text{HQ}]} = t(Q) \times \frac{K_H [\text{H}^+]}{1 + K_H [\text{H}^+]} \quad (30)$$

where Q is the grafted amine, K<sub>H</sub> is the apparent protonization constant. This fact points to the absence of the non-ideality effects. Also, these effects are negligible for all samples studied at the highest (within our study) temperature, 323 K.

For the rest of examined systems, the model of chemical reactions fitted the experimental data adequately if two reactions were taken into account\*, protonization of amines



and their homoconjugation



Irrespective of the support, the values of  $\log K_H$  are approximately linearly connected with the surface concentration of amines. The following regression equations were found (after the exclusion of sample 14 with the uniform surface topography):

$$\log K_H = 4.62 + 0.64 \cdot c_s \text{ (correlation coefficient } r = 0.88) \quad (33)$$

(primary amines, suspensions do not subjected to the heating–cooling cycle);

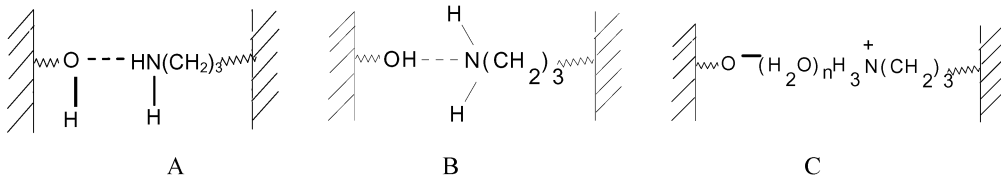
$$\log K_H = 5.59 + 0.60 \cdot c_s \text{ (} r = 0.97 \text{)} \quad (34)$$

(primary amines, suspensions were subjected to the heating–cooling cycle);

$$\log K_H = 6.53 + 0.25 \cdot c_s \text{ (} r = 0.94 \text{)} \quad (35)$$

(secondary amines, suspensions do not subjected to the heating–cooling cycle).

The  $K_H$  values are considerably smaller than the protonization constants of analogs in aqueous solutions, i.e., grafting decreases the basicity of amines. According to the NMR  $^{29}\text{Si}$  and  $^{13}\text{C}$  data [123] and results of molecular mechanics and quantum chemistry calculations [124], fixed amines interact with residual weak-acid silanol hydroxyls. These interactions result in the appearance of the system of hydrogen bonds or the salt-like products on the surface, for instance.



According to quantum-chemical simulations, structures A, B are more likely to form when the near-surface layer is water-deficient, while structure C corresponds to the full hydration of surface groups. Thus, it is impossible to consider the protonization constants as the characteristics of amines only. These constants describe protonization of amines together with bonded silanol hydroxyls [61].

The necessity to take into account the homoconjugation reactions was attributed to the interactions between neighbor grafted amino groups. Simulations performed with the use of calculated  $K_H$  and  $K_h$  values have shown that up to one-third of the total amount of amino groups forms homoconjugates  $\overline{HQ}_2^+$  [119]. As the average distance between grafted groups is large, the significant role of the homoconjugation reaction in the model suggests a nonuniform and non-random distribution of amino groups on the surface. A cluster (island-like) distribution of bonded groups [46,125] was finally concluded.

\*The used version of the model of chemical reactions is equivalent to the model of fixed bidentate centers with reactions shown in Fig. 3.

In any surface reaction, all phases remain electrically neutral. Obviously, it is necessary to take into account that protonization of grafted amines is accompanied by the penetration of counterions into the near-surface layer from the bulk of solution. Two simplified models were considered [61,119]. The first model assumes the free movement of counterions



where  $A^-$  is a counterion. The second model implies their strong fixation near the charged surface groups



where  $\eta_H$  is the mixed equilibrium constant expressed as

$$\eta_H = \frac{[\overline{QH^+} \overline{A^-}]}{[\overline{Q}] [\overline{A^-}] a_{H^+}} \quad (38)$$

the square brackets denote the equilibrium concentrations, and activity of the  $H^+$  ions in solution  $a_{H^+} = 10^{-pH}$ . The models differ also in the presentation of the homoconjugation reaction, assuming either the free movement of counterions or their fixation near the charged centers in the form of  $HQ^+ \overline{A^-}$ .

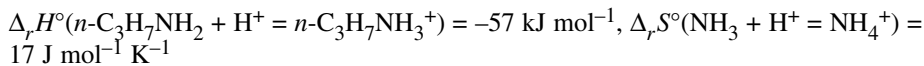
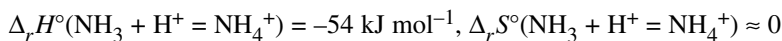
The simulations proved that the model of free movement failed to fit most of the  $H^+$  adsorption isotherms, while the model of strong fixation was adequate in the majority of cases. As the background electrolytes are present in great excess, their concentrations and the activity coefficients of all species remain practically constant, and  $[A^-]$  coincides with the initial concentration of the counterions ( $C$ ). This allows us to rewrite expression 38 as  $\eta_H = K_H / C$ . To determine the thermodynamic constant of reaction 37,  $\eta_H^T$ , it is necessary to extrapolate the  $\eta_H$  dependence on the concentration of the background electrolyte to zero ionic strength. Background electrolytes not only maintain a constant ionic strength (just as in studying equilibria in solutions) but also are the source of counterions and should be considered in this case as reagents too. To find the thermodynamic constants, the method using Pitzer's equations [126] for the calculation of activity coefficients of reagents in electrolyte solutions has been developed [114,127]. It was found that the type of the background electrolyte does not affect the value of  $\log \eta_H^T$ . For instance, for sample 12 (Table 1) at 293 K,  $\log \eta_H^T$  varies within the interval 7.2–7.4 for electrolytes  $NaNO_3$ ,  $KCl$ ,  $Na_2SO_4$ , and  $MgSO_4$ .

The models of chemical reactions and fixed polydentate centers (Table 2) describe adequately the experimental data without explicit consideration of the inter-ionic interactions in the near-surface layer. At the same time, it is evident that the inter-ionic interactions cannot be neglected because distances between likely charged ions on the surface (especially inside islands) are comparable with ones between likely charged ions in rather concentrated aqueous electrolyte solutions [128]. So, the background electrolyte does not shield completely the interactions between fixed ions. The only possible explanation was proposed in [128]: the surface charge is changed slightly at the change of composition of the near-surface layer, due to this the inter-ionic interactions give the constant contribution into energy of fixed ions and, consequently, the equilibrium constants do not depend on the extent of surface reactions (e.g., on the degree of protonization of grafted amines).

**Table 2** Parameters of the model of chemical reactions (293 K, ionic strength of solution is 0.1 mol L<sup>-1</sup>). Here and below, the values in brackets are the standard deviations of parameters.

No. of sample	Samples are not subjected to the heating–cooling cycle		Samples after the heating–cooling cycle
	$\log K_H$	$\log K_h$	
1	4.30 (0.03)	—	
2	5.34 (0.02)	2.4 (0.4)	
3	6.02 (0.04)	—	6.25 (0.01)
4	5.89 (0.06)	3.64 (0.18)	
5	5.35 (0.01)	2.8 (0.3)	
6	6.49 (0.03)	3.51 (0.05)	7.21 (0.08)
7	5.65 (0.11)	4.20 (0.15)	
8	7.81 (0.03)	2.97 (0.06)	7.50 (0.02)
9	7.11 (0.06)	—	7.15 (0.05)
10	6.50 (0.08)	3.42 (0.09)	7.13 (0.04)
11	6.82 (0.07)	2.87 (0.15)	6.97 (0.04)
12	6.65 (0.10)	3.72 (0.16)	6.81 (0.10)
13	6.89 (0.05)	—	
14	6.22 (0.05)	—	6.68 (0.15)
15	6.92 (0.07)	3.08 (0.05)	
16	6.90 (0.02)	—	
17	7.52 (0.07)	3.17 (0.18)	7.51 (0.08)
18	7.33 (0.07)	3.99 (0.09)	7.53 (0.20)
19	7.18 (0.10)	4.25 (0.15)	7.54 (0.20)

The  $\eta_H^T$  temperature dependence provides valuable information about the effects of hydration. Note in this connection that air-dry aminosilicas need to be kept out of the exiccator for 1–2 years to gain the properties of samples subjected to the heating–cooling cycle. The values of  $\log \eta_H^T$  depend on 1/T linearly (except data for the highest studied temperature 323 K) that allowed us to estimate the thermodynamic parameters of reaction 37:  $\Delta_r H^\circ \approx 10\text{--}20 \text{ kJ mol}^{-1}$ ,  $\Delta_r S^\circ \approx 175\text{--}200 \text{ J mol}^{-1} \text{ K}^{-1}$  [119]. They differ appreciably from parameters for the analogous reactions in aqueous solutions [55]:



The great entropy increase in reaction 37 and its endothermic character are connected with the partial loss of water molecules from the hydration shells of counterions when they penetrate into the near-surface layer. The gain in energy that accompanies the protonization process is surpassed by the consumption of energy necessary to the dehydration of counterions. In addition, the protonization of amino groups loosens the arching structure of the grafted layer and also leads to the entropy increase. The peculiarity observed for the  $\eta_H$  values at 323 K and the insignificance of the homoconjugation reaction at this temperature are due to the full hydration of the surface groups at this temperature (counterions penetrate into the near-surface layer without the loss of the water molecules).

In investigation of the biographic energetic heterogeneity (Table 3), properties of aminosilicas are considered from another standpoint [90]. For samples with small surface concentrations ( $c_s$ ) of amines, functions  $p(\log K_H)$  are unimodal. This points to the similar microenvironment of fixed amines. When  $c_s$  reaches the value about 1.5–1.8  $\mu\text{mol m}^{-2}$ , density functions  $p(\log K_H)$  become bimodal with the first peak coinciding in the position with the peak of unimodal functions. The treat-

ment of aminosilicas with minor silanizing reagents (samples 4 and 13) does not affect appreciably the density functions. The density function for sample 14 with the uniform surface distribution of amines differs significantly from functions for other samples and tends to the Dirac  $\delta$ -function. Exposing aminosilica samples to the heating–cooling cycle eliminates or decreases significantly the energetic heterogeneity.

**Table 3** Characteristics of the energetic heterogeneity of aminosilica samples (293 K, ionic strength of solution is 0.1 mol L<sup>-1</sup>).

No. of sample	Groups of different basicity			
	Position of the $p(K_H)$ maximum	Fraction	Position of the $p(K_H)$ maximum	Fraction
Samples are not subjected to the heating–cooling cycle				
1	4.66	1.0		
2	5.42	1.0		
3	6.33	1.0		
4	3.7	0.2	6.17	0.8
5	~4.8	0.4	5.78	0.6
6	4.76	0.15	7.08	0.85
7	4.42	0.3	7.25	0.7
8	6.50	0.26	8.46	0.74
9			7.50	1.0
10	4.77	0.4	7.43	0.6
11	5.65	0.2	6.96	0.8
12	3.6	0.32	6.94	0.6
13			7.11	1.0
14			6.08	1.0
15	6.08	0.3	7.35	0.7
16	5.28	0.25	7.50	0.75
17	4.58	<0.15	7.85	>0.85
18	~6	0.5	8.59	0.5
19	5.65	<0.5	>8.2	>0.5
Samples after the heating–cooling cycle				
3	6.84	1.0		
8	7.81	1.0		
9	6.92	1.0		
10	6.79	1.0		
12	4.23	0.15	6.91	0.85
17	4.85	0.08	7.95	0.92
18	6.60	0.2	7.67	0.8

The presence of two peaks on density functions  $p(\log K_H)$  corroborates the conclusion about the formation of the non-random (island-like) surface topography of aminosilicas at high  $c_s$ . Inside-islands amino groups are grafted tightly, while the density of groups outside islands is low. Amino groups of the second type interact with surface silanol groups more readily, and their basicity is lower. Thus, the first peak of  $p(\log K_H)$  characterizes the protolytic properties of amines outside the islands, whereas the second one corresponds to the “inside-island” groups. The obtained data (Table 3) indicate that amines are predominantly located inside islands. This phenomenon is due to a higher probability for new aminosilane molecule to be grafted near a previously immobilized molecule [5]. This explanation is in line with the existence of only one peak of density functions characterizing samples with low  $c_s$ . At low

$c_s$ , islands only start to form and their differences from isolated groups are difficult to register. For these samples, the random topography is a good approximation. The treatment of aminosilicas with hydrophobizing agents, which interact only with residual silanols out of islands, does not affect grafted amines.

Interesting independent information about the state of the surfaces was obtained by probing aminosilicas with Reichardt's solvatochromic betaine indicators [129]. Aminosilicas 8, 12, and 14 have been probed by the standard Reichardt's indicator 2,6-diphenyl-4-(2,4,6-triphenylpyridinium-1-yl)phenolate (in aqueous solution  $pK_a = 8.64$ , in ethanol  $\lambda_{max} = 550$  nm [130]); results are discussed in [131]. Reichardt's betaine indicators are widely used as molecular probes due to their high sensitivity to the state of media: even a slight change in its parameters changes position, shape, and width of the light absorption bands. The protonated form of the standard Reichardt's indicator does not absorb light in the long-wave region and exhibits no solvatochromic effect.

Very broad absorption bands with maxima at 600–700 nm were observed for samples 8 and 12 with the deposited probe. This is evidence that grafted amino groups are situated in the near-surface layer in such a manner that, at least, part of the indicator molecules exist in the neutral form. The big width of the absorption bands indicates the diverse microenvironment of the probe in the near-surface layer. Spectra of the probe sorbed by samples 12 and 14 have additional maxima at 450–500 nm that point to the existence of surface regions with substantially different polarities and acidities. At the same time, narrower bands in the absorption spectra of sample 14, which has amino groups uniformly distributed on the surface, testify that the diversity of the microenvironment of adsorbed probes diminishes. One of the most important results is the fact that the color of the sorbed probe appears only after the surface concentration of the indicator exceeds some threshold value in the range 0.02–0.06  $\mu\text{mol m}^{-2}$ . This corroborates the existence of regions with different acidities of the near-surface layer. At low surface concentrations, molecules of indicator cover surface regions with higher acidity and are transformed into the protonated (non-absorbing) form. Regions with lower acidity are covered only in the second turn. Similar results have been reported in [132]: the standard Reichardt's indicator adsorbed on a silica gel surface modified with *n*-propylamine absorbs visible light only when its concentration exceeds 0.08  $\mu\text{mol m}^{-2}$ .

Results of probing aminosilicas with  $\text{H}^+$  ions and Reichardt's betaine indicators may be summarized as follows:

- the non-ideal sorption of  $\text{H}^+$  ions by aminosilicas is described adequately with the account of the homoconjugation of grafted amines and their energetic heterogeneity;
- the non-random (island-like) topography of the aminosilica surfaces and the interaction of grafted amines with residual surface silanols are the main factors affecting the structure of the near-surface layer and its polarity and acidity;
- the protonization of grafted amines is accompanied by the strong binding of counterions from a bulk solution;
- grafting results in the decrease of the amine basicity due to their interactions with the residual surface silanols; logarithms of the apparent protonization constants increase approximately linearly with the increase of the surface concentration of grafted amines; and
- the protonization reactions are endothermic and proceed with the increase of entropy due to peculiarities of the hydration state of the near-surface layer.

Some important phenomena were revealed in investigating the complex formation of transition-metal ions with grafted organic bases [monodentate amines, ethylenediamine (En), diethylenetriamine (Dien), 1,10-phenanthroline (Phen), 2,2'-bipyridyl (Bipy), 2- and 8-aminemethylquinoline (2- and 8-AMQ)] [4,61,70,72,114,133–140].

*Bis*-complexes  $\text{MQ}_2$  ( $\text{M}$  is a metal ion, charges are omitted) are predominantly formed on silica surfaces modified by monodentate amines (data for  $\text{Cu}^{2+}$  complexes are presented in Table 4 as an example). When the surface is hydrated completely, these complexes turn into complexes  $\text{MQ}$ . Thus-

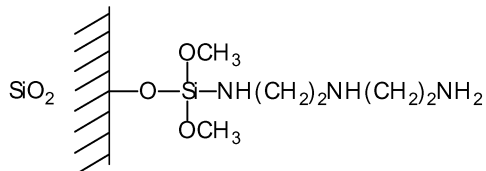
found composition of the fixed complexes is verified using their UV- and ESR-spectra. Stability constants of fixed complexes are close to stability constants of analogs in solutions and do not depend on the surface concentration of amines. In contrast to the complex formation reactions in solutions [141], reactions on surfaces are endothermic [142]. The order of stability constants corresponds to the Irving-Williams row:  $\text{Co}^{2+} \approx \text{Ni}^{2+} < \text{Cu}^{2+} > \text{Zn}^{2+}$ .

**Table 4** Logarithms of the apparent heterogeneous stability constants of the Cu(II) complexes with grafted monodentate amines (293 K, ionic strength of solution is 0.1 mol L<sup>-1</sup>).

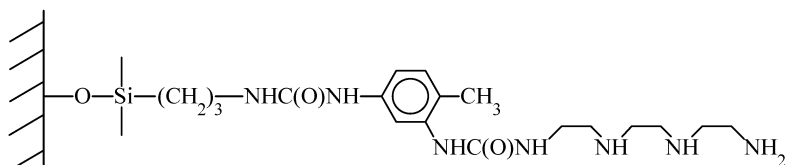
No. of sample	Samples are not subjected to the heating–cooling cycle		Samples after the heating–cooling cycle $\log \beta_1(\text{Cu}^{2+} + Q = \text{CuQ}^{2+})$
	$\log \beta_1(\text{Cu}^{2+} + Q = \text{CuQ}^{2+})$	$\log \beta_2(\text{Cu}^{2+} + 2Q = \text{CuQ}_2^{2+})$	
2		7.75 (0.05)	
5		7.92 (0.04)	
6		7.90 (0.02)	3.93 (0.10)
7		7.60 (0.20)	
8		7.83 (0.04)	
9		9.20 (0.10)	
14		7.18 (0.04)	
10	3.68 (0.04)		4.11 (0.03)
11		7.54 (0.01)	3.91 (0.02)
12	4.23 (0.03)		4.46 (0.03)
15		9.03 (0.05)	
17	4.24 (0.08)		
18		8.63 (0.07)	4.53 (0.02)
I		6.97	
II		6.98	
III		6.70	
IV		8.15	

I-IV: Silicas with grafted *n*-propylamine [97]; I, II: Silochromes C-80,  $c_s = 0.825$  and  $2.66 \mu\text{mol m}^{-2}$ , correspondingly; III: Silica gel,  $c_s = 4.78 \mu\text{mol m}^{-2}$ ; IV: Silochrome C-120,  $c_s = 5.58 \mu\text{mol m}^{-2}$ .

The comparative study of metal ions binding by different silica samples with grafted En and Dien clarified the influence of the leg type on the complexation [61,133,138]. For instance, when Dien is attached to the silica surface with a short leg



complex CuDien<sup>2+</sup> with  $\log \beta_1 = 9.80 \pm 0.10$  is formed. When Dien is attached with a longer leg



complex  $\text{CuDien}_2^{2+}$  is formed with  $\log \beta_2 = 5.88 \pm 0.13$ . In the latter case, Dien behaves as a bidentate ligand that is evident from the identity of UV-vis spectra of immobilized complexes  $\text{CuEn}_2^{2+}$  and  $\text{CuDien}_2^{2+}$  and the closeness of their stability constants.

An interesting finding is the coexistence of different complexes on the surface. For instance,  $\text{Cu}^{2+}$  forms complex  $\text{CuEn}^{2+}$ , and in slightly acidic medium a less stable complex  $\text{CuHEN}^{3+}$  starts to form; complexes  $[\text{CoEn}(\text{H}_2\text{O})_4]^{2+}$  with a distorted octahedral configuration and  $[\text{CoEn}(\text{H}_2\text{O})_2]^{2+}$  with the tetrahedral configuration also coexist on the surface [140].

The influence of solvents on the composition and stability of fixed complexes is a peculiar point. When silicas with grafted mono- and bidentate ligands adsorb metal salts from polar solvents (in which these salts are dissociated substantially), or salts have anions unable to form anionic metal complexes (such as perchlorate ions), *bis*-complexes  $\text{MQ}_2$  are predominantly formed. Results of simulation performed with the aid of models of chemical reactions and fixed bidentate centers (Tables 5 and 6) [61] point to the pronounced negative cooperativity effects. Also, stability constants of fixed complexes are decreased significantly as compared to their analogs in solutions. The preferred formation of *bis*-complexes is quite clear with the account of small distances between ligands within islands (island-like topography of the surfaces) and the formation of hydrogen bonds between grafted bases and surface residual silanols via the nitrogen donor atoms (Fig. 3). The presence of hydrogen bonds decreases the complexing ability of the ligands. At the same time, the *bis*-complexes are formed without any significant change of ligand positions, and in some cases are stabilized by the coordination bonds between the metal ion and the surface silanol groups. The negative cooperativity effect (low stability of complexes of equimolar M:Q composition) is accounted by the fact that ligands within islands are grafted tightly and the formation of complexes requires their partial detachment.

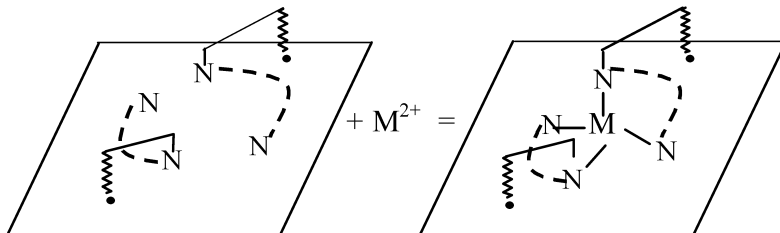


**Fig. 3** Schematic representation of formation of *bis*-complexes without detachment of the grafted reagents from the surface.

It was revealed also that, in contrast to solution equilibria, the stability constants of fixed complexes are affected mainly by the acceptor rather than donor properties of a solvent, and corresponding linear correlations were found [61]. For example,  $\log \beta_2 (\text{CuCl}_i^{(2-i)+} + 2\text{Bipy} = [\text{Cu}(\text{Bipy})_2]\text{Cl}_i^{(2-i)+}) = 9.1 + 1.6 E^N$ , where  $i = 0, 1, 2$  depending on a solvent (see notes to Table 5),  $E^N$  is the normalized Dimroth-Reichardt  $E_T$ -value [143,144] (the linear correlation of  $E_T$  and Gutmann's acceptor numbers was reported [130,145] that allows us to consider  $E_T$  as the measure of the acceptor ability of a solvent). The relatively lower stability of complexes in solvents with low  $E^N$  is due to the interactions of the grafted reagents with nondissociated chlorides; as a result of this reaction, chloride ions are driven, at least partially, from the inner to the outer sphere of the coordination compound.

**Table 5** Results of simulation of complexation equilibria on silica surfaces modified by Phen and Bipy with the aid of the model of chemical reactions.<sup>a</sup>

Solvent	Logarithms of heterogeneous stability constants <sup>b</sup>					
	$\overline{[\text{Cu}(\text{Bipy})_2\text{Cl}^{(1-i)+}]}$	$\overline{[\text{Cu}(\text{Bipy})_2\text{Cl}^{(1-i)+}]}$	$\overline{[\text{Co}(\text{Bipy})_2\text{Cl}_i^{(2-i)+}]}$	$\overline{[\text{Co}(\text{Bipy})_2\text{Cl}_i^{(2-i)+}]}$	$\overline{[\text{Cu}(\text{Phen})_2\text{Cl}_i^{(2-i)+}]}$	$\overline{[\text{Cu}(\text{Phen})_2\text{Cl}_i^{(2-i)+}]}$
Acn	16.06 (0.15)					16.26 (0.10)
Acl	9.82 (0.02)	13.41 (0.11)	9.39 (0.25)	15.91 (0.20)	21.3 (0.3)	15.02 (0.20)
PC	10.21 (0.01)	13.77 (0.04)	9.43 (0.03)	12.2 (0.4)	16.4 (0.20)	14.79 (0.15)
DMSO	9.47 (0.03)				9.50 (0.05)	14.50 (0.20)
Meth	10.54 (0.15)	14.82 (0.15)	9.76 (0.04)		9.55 (0.20)	13.18 (0.10)
DMSO	19.25 (0.06)		8.71 (0.03)		9.95 (0.15)	
Water	10.63 (0.03)		10.51 (0.03)		9.73 (0.03)	
					9.32 (0.03)	

<sup>a</sup>The following reactions were included into the models  $2\text{MCl}_i + 2\text{Q} = [\text{MQ}_2\text{Cl}_i^{(2-i)+}]$ ,  $\overline{\text{MCl}_i^{(2-i)+}} + \overline{\text{Q}} = \overline{\text{MQ}_2\text{Cl}_i^{(2-i)+}}$ ,  $i = 2$  for acetone (Acn), acetonitrile (Acl), and 1,2-propanediol (PC);  $i = 0$  for water and dimethylsulfoxide (DMSO);  $i = 0, 1, 2$  for dimethylformamide (DMFA) and methanol (Meth), Q is Phen or Bipy.

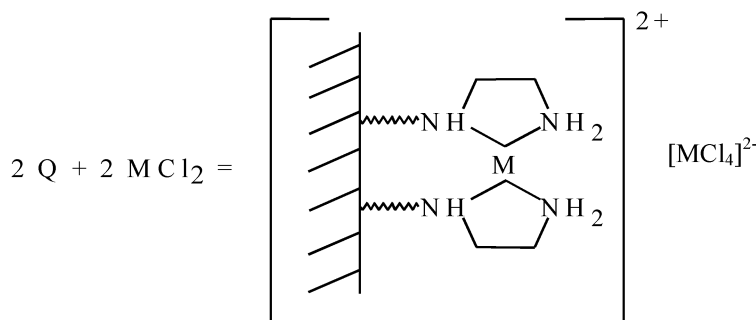
<sup>b</sup>For the correct comparison of data for different solvents, the reactant concentrations were expressed in molar fractions in calculating stability constants.

**Table 6** Results of simulation of complexation equilibria on silica surfaces modified by 2- and 8-AMQ with the aid of the model of fixed bidentate centers.<sup>a</sup>

Solvent	Logarithms of heterogeneous stability constants			
	CuCl <sub>2</sub> -2-AMQ		CuCl <sub>2</sub> -8-AMQ	
	log σ <sub>1</sub> <sup>(2)</sup>	log σ <sub>2</sub> <sup>(2)</sup>	log σ <sub>1</sub> <sup>(2)</sup>	log σ <sub>2</sub> <sup>(2)</sup>
Acl	3.74 (0.20)	7.06 (0.15)	4.00 (0.08)	6.79 (0.10)
PC	3.71 (0.09)	7.13 (0.08)	3.31 (0.10)	6.47 (0.07)
Meth	4.73 (0.04)	6.82 (0.06)		
DMFA	3.70 (0.06)	~5 (0.7)	2.94 (0.11)	4.25 (0.4)
DMSO	3.90 (0.10)		2.73 (0.04)	
Water	3.08 (0.05)		2.47 (0.04)	
CoCl <sub>2</sub> -2-AMQ				
CoCl <sub>2</sub> -8-AMQ				
	log σ <sub>1</sub> <sup>(2)</sup>	log σ <sub>2</sub> <sup>(2)</sup>	log σ <sub>1</sub> <sup>(2)</sup>	log σ <sub>2</sub> <sup>(2)</sup>
Acn	3.64 (0.09)	7.22 (0.04)	3.9 (0.3)	7.52 (0.18)
Acl	4.95 (0.20)	8.23 (0.20)	3.93 (0.10)	7.33 (0.15)
PC			3.56 (0.20)	~6 (0.4)
Meth	2.95 (0.03)			
DMFA	3.67 (0.06)		2.79 (0.06)	
DMSO	2.58 (0.05)		2.64 (0.03)	

<sup>a</sup>The following reactions were included into the models  $2\text{MCl}_2 + \overline{(\text{Q}_2)}^{\sigma_2^{(2)}} = \overline{[\text{MQ}_2][\text{MCl}_4]}^{\sigma_i^{(2)}} + \overline{(\text{Q}_2)}^{\sigma_i^{(2)}} = \text{MQ}_2\text{Cl}_i^{(2-i)+}$ ,  $i = 2$  for Acn, Acl, and PC;  $i = 0$  for water and DMSO;  $i = 0, 1, 2$  for DMFA and Meth, Q is 2- or 8-AMQ.

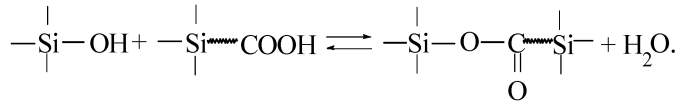
When metal chlorides are adsorbed from solvents with low polarity and acceptor ability, fixed complexes of composition  $\text{M}_2\text{Q}_2\text{Cl}_4$  are formed [133]. Since the absorption bands with maxima at ~1000 nm, characteristic for tetrachloro anionic metal complexes, were detected, it was concluded that the formation of coordination compounds on the surface was accompanied by the  $[\text{MCl}_4]^{2-}$  fixation in the form of counterions, for instance



## PROPERTIES OF ACIDS GRAFTED ON SILICA SURFACES

Many-years investigations of carbonic acids grafted on silica surfaces [95,96,146,147] did not provide clear understanding of factors affecting their protolytic and complexing properties because different ex-

perimental techniques gave significantly different results. Hydrogen bonds between carboxylic and silanol groups do not arise, and the interaction takes place only in vacuum at 140 °C [147]:



Thus, it is difficult to achieve the arching structures on the surface of carboxyl-containing silicas and the strong fixation of counterions.

To understand better the main features of these objects, a detailed study of macroporous silica with the grafted propionic acid (specific concentration 0.20 mmol g<sup>-1</sup>) was performed [148]. The pH-metric titration of suspensions of the material in aqueous solutions of NaCl, NaNO<sub>3</sub>, Na<sub>2</sub>SO<sub>4</sub>, and KNO<sub>3</sub> by an alkali solution was performed. Logarithms of apparent dissociation constants ( $K^\alpha$ ) were estimated as

$$\log K^\alpha = -\text{pH} + \lg \frac{\alpha}{1-\alpha} \quad (39)$$

where the degree of ionization  $\alpha = [\overline{\text{Q}}^-]/t(\text{HQ})$ . For background electrolytes KNO<sub>3</sub> and Na<sub>2</sub>SO<sub>4</sub>, the values of  $K^\alpha$  do not depend on  $\alpha$ , for NaCl  $K^\alpha$  increases in the range  $0 < \alpha < 0.5$ , and for NaNO<sub>3</sub> the values of  $K^\alpha$  decrease with the increase of  $\alpha$  (Fig. 4). Such different tendencies observed for the 1:1 electrolytes make it impossible to attribute the detected cooperative effects to the electrostatic interactions.

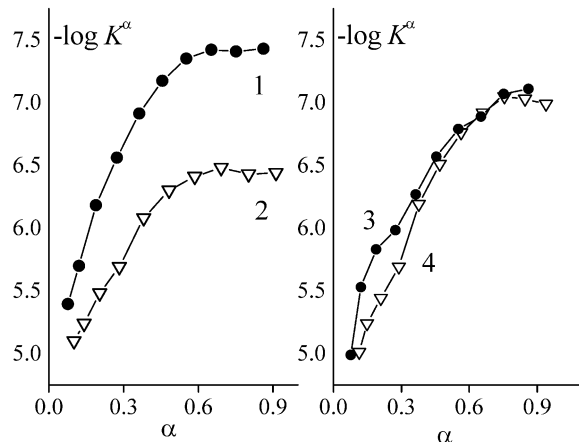


**Fig. 4** Dependencies of  $\log K^\alpha$  on  $\alpha$ . Background electrolytes:  $0.10 \text{ mol L}^{-1} \text{ NaCl}$  (1);  $0.75 \text{ mol L}^{-1} \text{ NaCl}$  (2);  $0.10 \text{ mol L}^{-1} \text{ NaNO}_3$  (3);  $0.30 \text{ mol L}^{-1} \text{ NaNO}_3$  (4).

Experimental data are adequately described with the model of chemical reactions, which includes reactions of two types



where  $\text{Cat}^+$  is a counterion and  $\chi$  and  $\omega$  are the equilibrium constants. Besides, to take into account the electrostatic effects, the volume of the adsorption (near-surface) layer  $V_{\text{ads}}$  was permitted to depend on  $\alpha^*$ :

$$V_{\text{ads}} = k \cdot \alpha_\gamma \quad (42)$$

where  $k$  is a constant. It was shown that

$$\log K^\alpha = B - (1 - \gamma) \cdot \log \alpha \quad (43)$$

where  $B = \log \frac{\omega \cdot t(\text{Cat}^+) \cdot k}{t(\text{HQ}) \cdot a}$ ,  $t(\text{Cat}^+)$  is the initial (total) molar concentration of the counterions,  $t(\text{HQ})$

is the specific concentration of carboxyl groups,  $a$  is the weight of the material. At fixed  $a$  and  $t(\text{Cat}^+)$ , coefficient  $B$  is constant, and the linear dependence between  $\log K^\alpha$  and  $\log \alpha$  exists. In testing the model for background electrolytes  $\text{NaCl}$  and  $\text{NaNO}_3$ , it was demonstrated that  $\log K^\alpha$  depends linearly on  $\log \alpha$  in the range  $-1.2 < \log \alpha < 0$  (correlation coefficients  $r = 0.97$ – $0.995$ , see Fig. 5),  $\gamma \approx -1$ , and

$$V_{\text{ads}} \approx k/\alpha \quad (44)$$

Most likely, expression 44 is valid only in a certain range of  $\alpha$ . The general expression should take into account both the increase of  $V_{\text{ads}}$  with the increase of the surface concentration of charged groups and its decrease due to the exclusion of water molecules from the near-surface layer by penetrating counterions. The results of simulations are summarized in Table 7. From the concentration dependence of mixed equilibrium constants  $\chi$ , the thermodynamic constants  $\chi^T$  were estimated,  $\log \chi^T$  were equal to  $-4.82$  ( $\text{Na}_2\text{SO}_4$ ) and  $-4.85$  ( $\text{KNO}_3$ ).

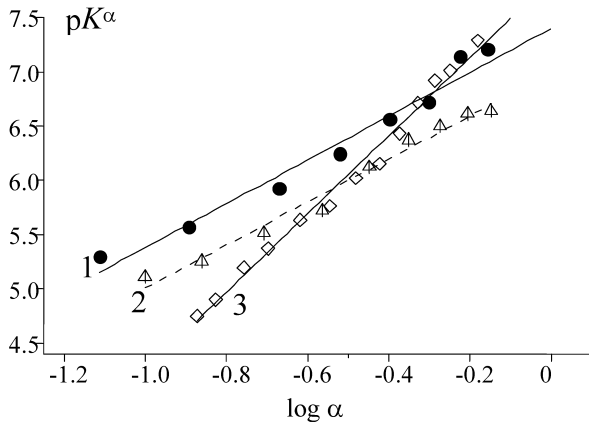


**Fig. 5** Dependencies of  $\log K^\alpha$  on  $\log \alpha$ . Background electrolytes:  $0.05 \text{ mol L}^{-1}$   $\text{NaCl}$  (1);  $0.75 \text{ mol L}^{-1}$   $\text{NaCl}$  (2); and  $0.50 \text{ mol L}^{-1}$   $\text{NaNO}_3$  (3).

\*The  $V_{\text{ads}}$  value was earlier supposed to depend on the specific surface area [61], the solution volume (in the presence of the long-range action [149]), and the bulk concentration of a sorbate [150].

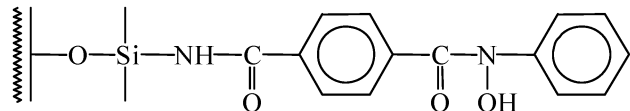
**Table 7** Parameters of the model of chemical reactions for protolytic equilibria of grafted propionic acid.

$t(M^+)$ , mol L <sup>-1</sup>	$-\log \omega^a$	$-\log \chi$	$t(M^+)$ , mol L <sup>-1</sup>	$-\log \omega^a$	$-\log \chi$
Background electrolyte Na <sub>2</sub> SO <sub>4</sub>					Background electrolyte NaCl
0.05	4.1 (0.4)	4.77 (0.09)	0.05	5.71 (0.07)	
0.10		4.69 (0.06)	0.10	6.26 (0.05)	
0.25		4.71 (0.03)	0.25	6.14 (0.10)	
0.40		4.93 (0.08)	0.40	6.54 (0.08)	
0.60		5.53 (0.14)	0.60	6.75 (0.02)	
0.75		5.52 (0.08)	0.75	6.42 (0.07)	
1.00		5.60 (0.09)	1.00		5.00 (0.05)
Background electrolyte KNO <sub>3</sub>					Background electrolyte NaNO <sub>3</sub>
0.05	3.3 (0.5)	4.77 (0.15)	0.10	5.78 (0.04)	
0.10		4.12 (0.08)	0.25	6.28 (0.08)	
0.25		3.81 (0.10)	0.30	6.17 (0.08)	
0.40		4.28 (0.09)	0.50	5.71 (0.08)	
0.60		4.16 (0.11)	0.60	6.06 (0.10)	
0.75		4.40 (0.01)	1.00	5.81 (0.01)	
1.00		4.48 (0.11)			

<sup>a</sup>Calculated for  $k = 3 \cdot 10^{-5}$  L.

When carboxyl groups dissociate, counterions are fixed strongly near the charged surface groups or migrate freely in the near-surface layer depending on type and concentration of the background electrolyte. The different behavior of counterions supplied by background electrolytes of the same type (free movement in the case of NaCl and NaNO<sub>3</sub>, strong fixation in the case of KNO<sub>3</sub>) originates from the differences in the hydration shells of Na<sup>+</sup> and K<sup>+</sup> ions. The hydration numbers of Na<sup>+</sup> were found to be 5 to 9, while for K<sup>+</sup> the values 2 to 5 were reported; the standard enthalpies of hydration were estimated as -430 to -470 kJ mol<sup>-1</sup> for Na<sup>+</sup> and -340 to -405 kJ mol<sup>-1</sup> for K<sup>+</sup> [151]. Due to the great size of the hydrated Na<sup>+</sup> cation, interactions of ionized carboxyl groups with counterions is weakened, and counterions become mobile, while in the case of smaller K<sup>+</sup> ions the electrostatic interactions are able to keep counterions near charged surface centers. As follows from the models of the double electric layer (DEL) [149], the increase of the cation and/or anion charges at the same equivalent concentrations gives rise to the drastic decrease of the DEL width. So, when NO<sub>3</sub><sup>-</sup> and Cl<sup>-</sup> ions are replaced by SO<sub>4</sub><sup>2-</sup> ions, the width of DEL decreases, and cations Na<sup>+</sup> and K<sup>+</sup> lose their mobility.

Whereas grafting does not affect the strength of carboxylic acids, the results of some early works allow us to suppose that very weak acids become stronger [152]. To elucidate this question, properties of Silochrome and Aerosil samples modified with *N*-benzoyl-*N*-phenylhydroxylamine (BPNA)



were investigated [153]. The protolytic properties of the surface groups were studied at 293 K and concentrations of the background electrolyte KCl in the range 0.1 to 1 mol L<sup>-1</sup>. The grafted BPNA groups differed significantly in their acidity (Fig. 6), the shape of density functions being independent on the ionic strength. These facts can be understood with the account of the chemical heterogeneity of surfaces resulting from the incomplete transformation of amino groups into the target BPNA groups. The small-

est dissociation constants ( $7 < pK_a < 9$ ) characterize the BPNA molecules grafted inside the islands with a rather high degree of transformation. The acidity of these BPNA molecules is the same as that of native analogs ( $pK_a = 8\text{--}9$ ) [154]. Some of the BPNA molecules are surrounded by grafted amines. Thus, the near-surface layer resembles, to a degree, basic solvents; BPNA dissociates easier; and  $pK_a < 5$ . At last, about one-quarter of BPNA molecules are out of islands and are characterized by  $pK_a = 5\text{--}7$ .

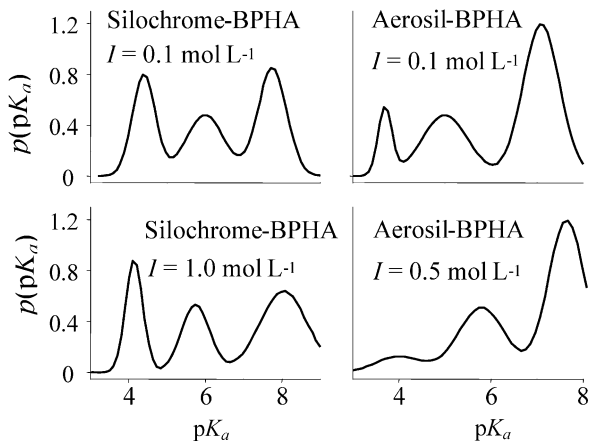
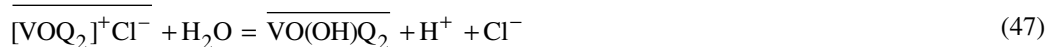


**Fig. 6** Distributions of grafted BPNA molecules in the  $pK_a$  values.

The dependence of the adsorption of metal salts on pH (Fig. 7) was the base for the determination of the composition and stability of fixed complexes. While in aqueous solutions metal ions form complexes including one, two, or three BPNA anions, the composition of complexes on the surface is much poorer: predominantly equimolar complexes are formed. The complexation reactions are as follows:



where  $\text{M}^{x+} = \text{Mn}^{2+}, \text{Ni}^{2+}, \text{Co}^{2+}, \text{Cu}^{2+}, \text{Zn}^{2+}, \text{Cd}^{2+}, \text{Pb}^{2+}$ , and  $\text{Fe}^{3+}$ ,  $\text{Q}^-$  is the BPNA anion,



The relationship between  $\log \beta_{11}$  and logarithms of constants of equilibria in water-dioxane mixtures (volume fraction of dioxane 50 %) at 298 K is practically linear:

$$\log \beta_{11} = \log \beta(\text{solution}) - 2.9 \quad (48)$$

Therefore, the immobilization results not only in the degeneration of the stoichiometry of complexes, but also in the decrease of their thermodynamic stability.

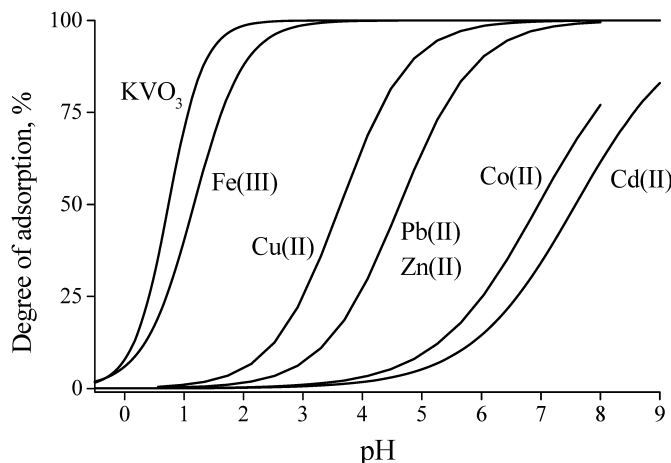


**Fig. 7** Examples of adsorption isotherms of metal ions (Silochrome-BPHA; 293 K).

### PROPERTIES OF AMPHOLYTES GRAFTED ON SILICA SURFACES

Basicity of grafted amines is decreased in comparison with native analogs because of the interaction with residual silanol groups; acidity of very weak acids, such as BPHA, is increased in the presence of unmodified surface amino groups. The question arises: Is it possible for species containing simultaneously basic and acidic groups to retain their protolytic and complexing properties at grafting? To answer this question, such grafted ampholytes as iminodiacetic acid (IDA), aminophosphonic acid (APA), and several aminodiphosphonic acids (ADPA) were studied by means of QPCA [155–160].

In the region of  $\text{pH} < 8$ , when the silica support remains stable, the adequate fit of the pH-titration data was provided by the model, taking into account only the first step ionization of IDA ( $\text{H}_2\text{Q}$ ):



the calculated  $\text{p}K_{\text{a}1}$  values at 293 K being equal to  $2.28 \pm 0.05$ ,  $2.25 \pm 0.05$ ,  $2.70 \pm 0.05$ , and  $3.14 \pm 0.03$  for ionic strengths of solution 0.10, 0.25, 0.50, and 1.00 mol L<sup>-1</sup>, respectively. These values are close to  $\text{p}K_{\text{a}1}$  of native analogs in aqueous solutions [161]. The compositions of iminodiacetate-metal ion complexes are the same as in solutions, though grafting decreases the difference between the stability constants of complexes formed by different metals.

Approximately the same results were obtained for silicas with grafted APA: fixation of the acid does not change its protolytic properties:  $\text{p}K_{\text{a}1} = 5.41$  vs.  $\text{p}K_{\text{a}1} = 5.31$  in aqueous solution [154]. At the same time, the adequate description of the experimental data required to include in the model the homoconjugation reaction describing the interactions of neighboring fixed species which are evidence of the island-like topography of grafting.

The ADPA-SiO<sub>2</sub> samples were prepared from aminosilicas by surface-assembling reactions, the yield of which never reaching 100 %. The degree of transformation of surface amines to ADPA ( $\tau$ , %) varied from 60 to 90 %. The dissociation constants of grafted ADPA are decreased significantly in comparison with the corresponding values for analogs in aqueous solutions. The higher the step of dissociation, the greater the difference. For instance, for grafted aminodi(methylphosphonic) acids,  $\text{p}K_{\text{a}1} < 2.6$ ;  $\text{p}K_{\text{a}2} = 5.2\text{--}6.2$ ;  $\text{p}K_{\text{a}3} = 7.3\text{--}8.2$ , while for its homogeneous analog, *N*-ethyliminodi(methylphosphonic) acid,  $\text{p}K_{\text{a}2} = 4.68$  and  $\text{p}K_{\text{a}3} = 5.92$  [162]. No correlation was found between  $\text{p}K_{\text{a}}$  and the surface con-

centrations of ADPA (in contrast to a linear dependence observed for aminosilicas). But the influence of the residual amino groups was revealed: there is a linear correlation between  $pK_{a2}$  and  $\tau$ :

$$pK_{a2} = 8.8 - 0.04\tau \quad (50)$$

It can be estimated from the above equation that  $pK_{a2} = 4.8$  in the ideal case of the complete transformation of surface amino groups to ADPA. This value is very close to  $pK_{a2}$  for the native analog, which suggests no significant chemical interactions between grafted ADPA and silanols and means that no other physical phenomena reduce the acidity of bonded groups except their interaction with residual amines. Similar analysis of  $pK_{a3}$  values shows their correlation with the concentration of surface silanols.

AP and ADPA form stable complexes with *s*-, *p*-, *d*- and *f*-metal ions, including protonated and polynuclear ones; complexes of rare-earth and many transition metals are insoluble [162–164]. The dependencies of adsorption of metal ions by different APA-SiO<sub>2</sub> and ADPA-SiO<sub>2</sub> samples on pH and initial concentrations of reagents were the source for the determination of stoichiometric composition (Table 8) and heterogeneous stability constants of fixed complexes.

Grafted APA and ADPA form complexes with the equimolar amounts of acids and metal ions, complexes with Fe(III), Cu(II), Pb(II), and *f*-metal ions being the most stable. As distinct from the complexation in solutions, polynuclear complexes are not formed. The fixed ADPA complexes are more stable than their analogs in solutions. Though the information about stability of complexes formed by ADPA in solutions is rather poor, the existence of correlation between stability constants of fixed complexes and their soluble analogs was reported [155]. The decrease of the ADPA dissociation constants and the increase of stability of metal ion complexes were attributed to the interaction of grafted acids with residual amino groups. ADPA protonates amino groups (which become the “surface counterions”). Thus, additional (in comparison with native analogs in solutions at the same pH) negative charges appear in fixed ADPA groups.

**Table 8** Stoichiometric compositions of APA and ADPA complexes fixed on silica surface.

	APA (H <sub>2</sub> Q)	ADPA (H <sub>4</sub> Q)
Metal ions	La <sup>3+</sup> , Cd <sup>2+</sup> , Co <sup>2+</sup> , Ni <sup>2+</sup> , Cu <sup>2+</sup>	La <sup>3+</sup> , Cd <sup>2+</sup> , Mn <sup>2+</sup> , Co <sup>2+</sup> , Ni <sup>2+</sup> , Cu <sup>2+</sup> , Zn <sup>2+</sup>
Complexes	MHQ *, M(HQ) <sub>2</sub> , MQ *	MH <sub>2</sub> Q *, MHQ, M(H <sub>2</sub> Q) <sub>2</sub> *, M(HQ) <sub>2</sub>

M: metals. Complex charges are omitted. Symbol \* denotes the dominating complexes.

## ACKNOWLEDGMENT

The authors are deeply indebted to Prof. Alexander Korobov for his great help in preparing this manuscript.

## REFERENCES

1. D. E. Leyden, G. H. Luttrell. *Anal. Chem.* **47**, 1612 (1973).
2. J. W. Burgraf, D. S. Kendall, D. E. Leyden, F. J. Pern. *Anal. Chim. Acta* **129**, 19 (1981).
3. Y. Gushikem, M. A. A. da Silva. *J. Colloid Interface Sci.* **107**, 81 (1985).
4. V. V. Skopenko, V. N. Zaitsev, Yu. V. Kholin, A. A. Bugaevskii. *Russ. J. Inorg. Chem.* **32**, 970 (1987).
5. V. A. Tertykh, L. A. Belyakova. *Chemical Reactions Involving Silica Surface*, Naukova Dumka, Kiev (1991).
6. A. Mottula, J. R. Steinmetz (Eds.). *Chemically Modified Surfaces*, Elsevier, Amsterdam (1992).

7. J. F. Biernat, P. Konieczko, B. J. Tarbet, J. S. Bradshow. *Separation and Purification Methods*, Marcel Decker, New York, **23**, 77 (1994).
8. J. J. Pesek, M. T. Matuska, R. R. Abuelafya (Eds.). *Chemically Modified Surfaces. Recent Developments*, Royal Society of Chemistry, Cambridge (1996).
9. A. Dabrowski, V. A. Tertykh (Eds.). *Adsorption on New and Modified Inorganic Sorbents*, Elsevier, Amsterdam (1996).
10. J. P. Blitz, C. B. Little (Eds.). *Fundamentals and Applied Aspects of the Chemically Modified Surfaces*, Royal Society of Chemistry, London (1999).
11. G. V. Lisichkin (Ed.). *Chemistry of Grafted Surface Compounds*, Fizmatlit, Moscow (2003).
12. A. Walcarius, V. Ganesan. *Langmuir* **22**, 469 (2006).
13. A. R. Cestari, E. F. S. Vieira, E. C. N. Lopes, R. G. da Silva. *J. Colloid Interface Sci.* **272**, 271 (2004).
14. N. R. E. N. Impens, P. van der Voort, E. F. Vansant. *Microporous Mesoporous Mater.* **28**, 217 (1999).
15. A. P. Wight, M. E. Davis. *Chem. Rev.* **102**, 3589 (2002).
16. P. K. Jal, S. Patel, B. K. Mishra. *Talanta* **62**, 1005 (2004).
17. R. M. Barabash, T. V. Kovalchuk, V. N. Zaitsev, H. Sfihi, J. Fraissard, *J. Phys. Chem. A* **107**, 4497 (2003).
18. C. T. Kresge, M. E. Leonowicz, W. J. Roth, J. C. Vartuli, J. S. Beck. *Nature* **359**, 710 (1992).
19. C. J. Brinker, G. W. Scherer. *Sol-Gel Science*, Academic Press, San Diego (1990).
20. M. A. Wahab, I. Imae, Y. Kawakami, C.-S. Ha. *Chem. Mater.* **17**, 2165 (2005).
21. A. K. Trofimchuk, V. A. Kuzovenko, I. V. Mel'nik, Yu. L. Zub. *Russ. J. Appl. Chem.* **79**, 229 (2006).
22. M. Etienne, A. J. C. Moreira, Y. Gushikem. *Anal. Chim. Acta* **176**, 2263 (1985).
23. P. N. Nesterenko, O. S. Zhukova, O. A. Shpigun, P. Jones. *J. Chromatogr. A* **813**, 47 (1998).
24. P. N. Nesterenko, M. J. Shaw, S. J. Hill, P. Jones. *Microchem. J.* **62**, 58 (1999).
25. M. K. Richmond, S. L. Scott, H. Alper. *J. Am. Chem. Soc.* **123**, 10521 (2001).
26. J. Clark, D. Macquarrie (Eds.). *Handbook of Green Chemistry and Technology*, Blackwell Science, Oxford (2002).
27. G. Zaitseva, Y. Gushikem, E. S. Ribeiro, S. S. Rosatto. *Electrochim. Acta* **47**, 1469 (2002).
28. M. M. Collinson. *Trends Anal. Chem.* **21**, 30 (2002).
29. E. S. Ribeiro, S. S. Rosatto, Y. Gushikem, L. T. Kubota. *J. Sol. State Electrochem.* **7**, 665 (2003).
30. A. Walcarius. *Talanta* **59**, 1173 (2003).
31. A. Walcarius, M. Etienne, S. Sayen, B. Lebeau. *Electroanalysis* **15**, 414 (2003).
32. L. Bois, A. Bonhomme, A. Ribes, B. Pais, G. Raffin, F. Tessier. *Colloids Surf., A* **221**, 221 (2003).
33. V. N. Zaitsev. *J. Anal. Chem.* **58**, 612 (2003).
34. G. P. Knowles, J. V. Graham, S. W. Delaney, A. L. Chaffee. *Fuel Process. Technol.* **86**, 1435 (2005).
35. H. Yoshitake, E. Koiso, H. Horie, H. Yoshimura. *Microporous Mesoporous Mater.* **85**, 183 (2005).
36. X. Wang, K. S. K. Lin, J. C. C. Chan, S. Cheng. *J. Phys. Chem. B* **109**, 1763 (2005).
37. A. Walcarius, D. Mandler, J. A. Cox, M. Collinson, O. Lev. *J. Mater. Chem.* **15**, 3663 (2005).
38. O. V. Gluschenko, E. S. Yanovska, O. Yu. Kichkiruk, V. A. Tertykh. *Funct. Mater.* **13**, 265 (2006).
39. M. M. Hassanien, S. A.-E.-S. Khaled. *Talanta* **68**, 1550 (2006).
40. L. He, C.-S. Toh. *Anal. Chim. Acta* **556**, 1 (2006).
41. V. S. Tripathi, V. B. Kandimalla, H. Ju. *Sens. Actuators, B* **114**, 1071 (2006).
42. O. Zaporozhets, O. Gawer, V. Sukhan. *Colloids Surf., A* **147**, 273 (1999).
43. A. Krysztafkiewicz, S. Binkowski, T. Jesionowski. *Appl. Surf. Sci.* **199**, 31 (2002).
44. R. P. Linnik, O. A. Zaporozhets. *Anal. Bioanal. Chem.* **375**, 1083 (2003).

45. E. F. Vansant, P. Van der Voort, K. C. Vrancken. *Characterisation and Chemical Modification of the Silica Surface*, Amsterdam, Elsevier (1995).
46. V. N. Zaitsev. *Complexing Silicas: Synthesis, Structure of Bonded Layer and Surface Chemistry*, Folio, Kharkov (1997).
47. A. Y. Fadeev, Yu. V. Kazakevich. *Langmuir* **18**, 2665 (2002).
48. C. J. Brinker, G. W. Scherer. *Sol–Gel Science: The Physics and Chemistry of Sol–Gel Processing*, Academic Press, San Diego (1990).
49. M. A. Wahab, W. Guo, W.-J. Cho, C.-S. Ha. *J. Sol–Gel Sci. Technol.* **27**, 333 (2003).
50. D. R. Azolin, C. C. Moro, T. M. H. Costa, E. V. Benvenutti. *J. Non-Cryst. Solids* **337**, 201 (2004).
51. W. Cheng, Z. Zhou, W. Miao, H. Chen, B. Huang, T. Tang. *Mater. Lett.* **60**, 1843 (2006).
52. N. Kurnakov. *Usp. Fiz. Nauk* **IV**, 339 (1924).
53. (a) D. Mendeleev. *Compounds of Ethyl Alcohol with Water*. In *Collected Works*, AN SSSR Publishing, Leningrad, **4**, 414 (1937); (b) D. Mendeleev. *Investigation of Aqueous Solutions by Specific Gravity*, St. Petersburg (1887).
54. (a) V. Ya. Anosov, M. I. Ozerova, Yu. Ya. Fialkov. *Fundamentals of Physicochemical Analysis*, Nauka, Moscow (1976); (b) Yu. Ya. Fialkov. *Physicochemical Analysis of Liquid Systems and Solutions*, Naukova Dumka, Kiev (1992).
55. (a) The IUPAC Stability Constants Database, SC-Database and Mini-SCDatabase (<<http://www.acadsoft.co.uk/scdbase/scdbase.htm>>); (b) NIST Critically Selected Stability Constants of Metal Complexes: Version 8.0 (<<http://www.nist.gov/srd/nist46.htm>>).
56. M. Meloun, J. Havel, E. Höglfeldt. *Computation of Solution Equilibria. A Guide to Methods in Potentiometry, Extraction and Spectrophotometry*, Ellis Horwood, Chichester (1987).
57. A. E. Martell, R. J. Motekaitis. *The Determination and Use of Stability Constants*, VCH, Weinheim (1988).
58. R. B. Hancock. *Analyst* **122**, 51R (1997).
59. M. Beck, I. Nagypal. *Chemistry of Complex Equilibria*, Akademiai Kiado, Budapest (1989).
60. A. I. Lesnikovich, S. V. Levchik. *Correlations in Modern Chemistry*, Universitetskoe, Minsk (1989).
61. Yu. V. Kholin. *Quantitative Physicochemical Analysis of Complexation in Solutions and on the Surface of Complexing Silicas: Meaningful Models, Mathematical Methods and their Application*, Folio, Kharkov (2000).
62. Y. A. Kokotov. *Zh. Fiz. Khim.* **69**, 2249 (1995).
63. A. A. Lopatkin, A. V. Vernov. *Zh. Fiz. Khim.* **69**, 2253 (1995).
64. V. B. Fainerman, D. Vollhardt. *J. Phys. Chem. B* **103**, 145 (1999).
65. A. I. Rusanov. *J. Phys. Chem. B* **110**, 3447 (2006).
66. V. B. Fainerman, D. Vollhardt. *J. Phys. Chem. B* **110**, 3448 (2006).
67. A. A. Lopatkin. *Theoretical Foundations of Physical Adsorption*, MGU Publishing, Moscow (1983).
68. A. A. Lopatkin. *Pure Appl. Chem.* **61**, 1981 (1989).
69. (a) V. B. Aleskovskii. *The Course of Chemistry of Supermolecular Compounds*, Leningrad State University, Leningrad (1990); (b) V. B. Aleskovskii. *Chemistry of Supermolecular Compounds*, St. Petersburg State University, St. Petersburg (1996).
70. Y. V. Kholin, V. N. Zaitsev, N. D. Donskaya. *Zh. Neorg. Khim.* **35**, 1569 (1990).
71. A. W. Adamson. *Physical Chemistry of Surfaces*, 5<sup>th</sup> ed., John Wiley, New York (1990).
72. V. V. Skopenko, Y. V. Kholin, V. N. Zaitsev, S. A. Meynii, D. S. Konyaev. *Russ. J. Phys. Chem.* **67**, 728 (1993).
73. Yu. V. Kholin. *Funct. Mater.* **2**, 23 (1995).
74. A. M. Evseev, L. S. Nikolaeva. *Zh. Fiz. Khim.* **67**, 508 (1993).
75. L. S. Nikolaeva, Yu. A. Kir'yanov. *Russ. J. Phys. Chem.* **71**, 659 (1997).

76. S. Z. Roginskii. *Adsorption and Catalysis on Heterogeneous Surfaces*, AN SSSR Publishing, Moscow (1948).
77. M. J. Jaycock, G. D. Parfitt. *Chemistry of Interfaces*, Ellis Horwood, Chichester (1981).
78. M. Jaroniec, R. Madey. *Physical Adsorption on Heterogeneous Solids*, Elsevier, Amsterdam (1988).
79. V. Sh. Mamleev, P. P. Zolotarev, P. P. Gladyshev. *Heterogeneity of Sorbents (Phenomenological Models)*, Nauka, Alma-Ata (1989).
80. M. Borcovec, B. Jönsson, G. J. M. Koper. In *Colloids Surf. Sci.*, E. Matijevic (Ed.), Plenum Press, New York, **16** (1999).
81. D. L. Sackett, H. A. Saroff. *FEBS Lett.* **397**, 1 (1996).
82. B. Perlmuter-Hayman. *Acc. Chem. Res.* **19**, 90 (1986).
83. A. Braibanti, E. Fisicaro, C. Comparti, A. Ghiozzi, R. S. Rao, G. N. Rao. *React. Funct. Polym.* **36**, 245 (1998).
84. H. S. Taylor. *J. Phys. Chem.* **30**, 145 (1926).
85. C. Contescu, J. Jagiello, J. A. Schwarz. *Langmuir* **9**, 1754 (1993).
86. H. S. Simms. *J. Am. Chem. Soc.* **48**, 1239 (1926).
87. A. A. Bugaevsky. *Dokl. Akad. Nauk SSSR* **161**, 140 (1965).
88. H. B. F. Dixon, S. D. Clarke, G. A. Smith, T. K. Carne. *Biochem. J.* **278**, 279 (1991).
89. (a) A. Tikhonov, A. Goncharsky, V. Stepanov, A. Yagola. *Numerical Methods for the Solution of Ill-Posed Problems*, Kluwer Academic, Dordrecht (1995); (b) A. Bakushinsky, A. Goncharsky. *Ill-Posed Problems: Theory and Applications*, Kluwer Academic, Dordrecht (1994).
90. Yu. Kholin, S. Myerniy, G. Varshal. *Adsorption Sci. Technol.* **18**, 267 (2000).
91. Yu. Kholin, S. Myerniy. *Kharkov Univer. Bull., Chem. Ser.* **11**, 351 (2004), <<http://www-chemistry.univer.kharkov.ua/rus/bulletin.php?num=626>>.
92. Y. Khoroshevskiy, S. Korneev, S. Myerniy, Y. V. Kholin, F. A. Pavan, J. Schifino, T. M. H. Costa, E. V. Benvenutti. *J. Colloid Interface Sci.* **284**, 424 (2005).
93. E. T. Jaynes. *Phys. Rev.* **106**, 620 (1957).
94. (a) A. P. Filippov. *Teor. Eksp. Khim.* **19**, 463 (1983); (b) A. P. Filippov. *Teor. Eksp. Khim.* **21**, 693 (1985).
95. G. V. Kudryavtsev, G. V. Lisichkin, V. M. Ivanov. *Zh. Anal. Khim.* **32**, 22 (1983).
96. G. V. Kudryavtsev. *Zh. Fiz. Khim.* **61**, 468 (1987).
97. G. V. Kudryavtsev, D. V. Milchenko, V. V. Yagov, A. A. Lopatkin. *J. Colloid Interface Sci.* **140**, 114 (1990).
98. A. M. S. Lucho, A. Panteleimonov, Y. Kholin, Y. Gushikem. *J. Colloid Interface Sci.* **310**, 47 (2007).
99. (a) U. P. Strauss, B. W. Barbieri, G. Wong. *J. Phys. Chem.* **83**, 2840 (1979); (b) U. P. Strauss. *Macromolecules* **15**, 1567 (1982).
100. (a) J. Bjerrum. *Metal Amine Formation in Aqueous Solution. Theory of the Reversible Step Reactions*, P. Haase, Copenhagen (1957); (b) B. Sen. *Anal. Chim. Acta* **27**, 515 (1962); (c) C. Tanford. *Physical Chemistry of Macromolecules*, Wiley Interscience, New York (1961).
101. F. R. Hartley, C. Burgess, R. M. Alcock. *Solution Equilibria*, Ellis Horwood, Chichester (1980).
102. A. A. Bugaevsky, Yu. V. Kholin. *Anal. Chim. Acta* **241**, 353 (1991).
103. V. I. Mudrov, B. L. Kushko. *Methods for Treatment of Measurements*, 2<sup>nd</sup> ed., Radio i Svyaz', Moscow (1983).
104. P. Huber. *Robust Statistical Procedures*. In *CBMS-NSF Regional Conf. Series in Appl. Mathematics*, SIAM, Philadelphia (1996).
105. I. Vuchkov, L. Boyadjieva, E. Solakov. *Applied Linear Regression Analysis*, Finansi i Statistika, Moscow (1987).
106. S. A. Merny, D. S. Konyaev, Yu. V. Kholin. *Kharkov Univ. Bull., Chem. Ser.* **420**, 112 (1998).

107. L. Sachs. *Statistische Auswertungsmethoden*, Springer, Berlin (1972).
108. (a) M. Stone. *J. Royal Stat. Soc.* **36**, 111 (1974); (b) D. W. Osten. *J. Chemom.* **2**, 39 (1988); (c) E. Bradley. *Am. Stat.* **37**, 36 (1983).
109. (a) L. Zekany, I. Nagypal. In *Computational Methods for the Determination of Formation Constants*, D. J. Legget (Ed.), pp. 291–353, Plenum Press, New York (1985); (b) P. Gans, A. Sabatini, A. Vacca. *Talanta* **43**, 1739 (1996).
110. C. L. Lawson, R. J. Hanson. *Solving Least Squares Problems*, Prentice-Hall, Englewood Cliffs (1974).
111. (a) T. Turanyi. *Comput. Chem.* **14**, 253 (1990); (b) T. Kovács, I. G. Zsély, A. Kramaries, T. Turányi. *J. Anal. Appl. Pyrol.* **79**, 252 (2007).
112. G. V. Kudryavtsev, S. Z. Bernadyuk, G. V. Lisichkin. *Russ. Chem. Rev.* **58**, 406 (1989).
113. Yu. V. Kholin, V. N. Zaitsev, S. A. Merny, N. D. Donskaya, L. N. Chistyakova. *Ukr. Khim. Zh.* **59**, 910 (1993).
114. Yu. V. Kholin, Yu. V. Shabaeva. *Russ. J. Appl. Chem.* **71**, 1524 (1998).
115. V. N. Zaitsev, V. D. Oleynik. *Adsorption Sci. Technol.* **17**, 65 (1999).
116. V. D. Oleynic, V. N. Zaitsev, V. L. Budarin. *Adsorption Sci. Technol.* **17**, 835 (1999).
117. A. A. Samoteikin, Yu. V. Kholin, V. N. Zaitsev, N. R. Sumskaya. *Funct. Mater.* **7**, 144 (2000).
118. S. A. Alexeev, V. N. Zaitsev, M. O. Genina. *Ukr. Khim. Zh.* **66**, 61 (2000).
119. Y. Kholin, S. Myerniy, Y. Shabaeva, I. Khristenko, A. Samoteikin, N. Sumskaya. *Adsorption Sci. Technol.* **21**, 53 (2003).
120. V. N. Zaitsev, N. G. Kobylinskaya. *Russ. Chem. Bull.* **54**, 1842 (2005).
121. T. Kovalchuk, H. Sfihi, L. Kostenko, V. Zaitsev, J. Fraissard. *J. Colloid Interface Sci.* **302**, 214 (2006).
122. (a) V. N. Zaitsev, V. V. Skopenko, Yu. V. Kholin, N. D. Donskaya, S. A. Merny. *Russ. J. Gen. Chem.* **60**, 529 (1995); (b) V. N. Zaitsev. In *Chemically Modified Surfaces. Recent Developments*, J. J. Pesek, M. T. Matuska, R. R. Abuelafya (Eds.), pp. 113–124, Royal Society of Chemistry, Cambridge (1996).
123. (a) G. S. Caravajal, D. E. Leyden, G. R. Quinting, G. E. Macielet. *Anal. Chem.* **60**, 1776 (1981); (b) D. E. Leyden, D. S. Kendall, T. G. Waddell. *Anal. Chim. Acta* **89**, 207 (1981); (c) S. Shimoda, Y. Saito. *J. Colloid Interface Sci.* **89**, 293 (1982).
124. (a) A. A. Golub, B. V. Zubenko. *J. Colloid Interface Sci.* **179**, 482 (1996); (b) Yu. Kholin, O. A. Zhikol, D. S. Konyaev, Yu. V. Shabaeva. *Kharkov Univ. Bull.* **532**, *Chem. Ser.* **7**, 44 (2001).
125. J. C. Hicks, C. W. Jones. *Langmuir* **22**, 2676 (2006).
126. (a) K. S. Pitzer. *J. Phys. Chem.* **77**, 268 (1973); (b) K. S. Pitzer, G. J. Mayorga. *J. Phys. Chem.* **77**, 2300 (1973).
127. Yu. V. Kholin, A. A. Bugaevskii, D. S. Konyaev, Yu. V. Shabaeva. *Ukr. Chem. J.* **65**, 110 (1999).
128. A. V. Vernov, A. A. Lopatkin. *Zh. Fiz. Khim.* **63**, 1909 (1989).
129. C. Reichardt. *Pure Appl. Chem.* **76**, 1903 (2004).
130. C. Reichardt. *Solvents and Solvent Effects in Organic Chemistry*, 3<sup>rd</sup> updated and enlarged ed., Wiley-VCH, Weinheim (2003).
131. I. V. Khristenko, Yu. V. Kholin, N. O. Mcchedlov-Petrossyan, C. Reichardt, V. N. Zaitsev. *Colloid J.* **68**, 511 (2006).
132. D. J. Macquarrie, S. J. Tavener, G. W. Gray, P. A. Heath, J. S. Rafelt, S. I. Saulzet, J. J. E. Hardy, J. H. Clark, P. Sutra, D. Brunel, F. di Renzo, F. Fajula. *New J. Chem.* **23**, 725 (1999).
133. T. P. Lishko, L. V. Gluschenko, Yu. V. Kholin, V. N. Zaitsev, N. D. Donskaya. *Zh. Fiz. Khim.* **65**, 2996 (1991).
134. V. N. Zaitsev, V. V. Skopenko, L. V. Gluschenko. In *Chemically Modified Surfaces*, A. Mottula, J. R. Steinmetz (Eds.), p. 397, Elsevier, Amsterdam (1992).
135. V. N. Zaitsev, Yu. V. Kholin, D. S. Konyaev. *Russ. J. Inorg. Chem.* **38**, 947 (1993).

136. Yu. V. Kholin, V. N. Zaitsev, S. A. Merniy, O. A. Varzatsky. *Russ. J. Inorg. Chem.* **40**, 1325 (1995).
137. V. N. Zaitsev, V. D. Oleynic, V. V. Skopenko, V. V. Antoschuk. *Funct. Mater.* **2**, 69 (1995).
138. Yu. V. Kholin. *Russ. J. Inorg. Chem.* **41**, 440 (1996).
139. Yu. V. Kholin, I. V. Khristenko, Yu. V. Shabaeva, N. R. Sumskaya. *Russ. J. Inorg. Chem.* **43**, 75 (1998).
140. V. N. Zaitsev, Yu. V. Kholin, I. V. Khristenko, Yu. V. Shabaeva. *Kharkov Univ. Bull.* **437**, *Chem. Ser.* **3**, 156 (1999).
141. V. P. Vasilyev, V. A. Borodin. *Russ. J. Inorg. Chem.* **35**, 259 (1990).
142. Yu. V. Kholin, I. V. Khristenko. *Kharkov Univ. Bull.* **596**, *Chem. Ser.* **10**, 171 (2003).
143. U. Mayer, V. Gutmann, W. Gerger. *Monatsh. Chem.* **106**, 1235 (1975).
144. J. Burgess. *Pure Appl. Chem.* **63**, 1677 (1991).
145. Yu. Ya. Fialkov. *Solvent as a Tool for Control over Chemical Processes*, Khimiya, Leningrad (1990).
146. (a) G. V. Kudryavtsev, G. V. Lisichkin. In *Adsorption and Adsorbents*, **12**, pp. 33–39, Naukova Dumka, Kiev (1984); (b) D. V. Milchenko, G. V. Kudryavtsev. *Teor. Eksp. Khim.* **22**, 243 (1986); (c) D. V. Milchenko, G. V. Kudryavtsev, G. V. Lisichkin. *Zh. Fiz. Khim.* **60**, 2361 (1986); (d) S. S. Silchenko. Ph.D. thesis, Kiev (1993).
147. G. V. Lisichkin, G. V. Kudryavtsev. In *5<sup>th</sup> Int. Symp. on Connection between Homogeneous and Heterogeneous Catalysis*, **2**, Part 1, pp. 84–103, Novosibirsk (1986).
148. Yu. V. Kholin, Yu. V. Shabaeva. *Funct. Mater.* **6**, 131 (1999).
149. B. V. Derjagin, N. V. Churaev, V. M. Muller. *Surface Forces*, Consultants Bureau, New York (1987).
150. D. V. Marinin, A. P. Golikov, A. V. Voit, V. A. Avramenko, V. Yu. Glushchenko. *J. Colloid Interface Sci.* **152**, 161 (1992).
151. M. Bakeev. *Theory of Hydration and Dissolution of Salts*, Nauka, Alma-Ata (1990).
152. (a) T. I. Vertinskaya, G. V. Kudryavtsev, T. I. Tikhomirova, V. I. Fadeeva. *Zh. Anal. Khim.* **40**, 1387 (1985); (b) I. B. Yuferova, G. V. Kudryavtsev, T. I. Tikhomirova, V. I. Fadeeva. *Zh. Anal. Khim.* **43**, 1643 (1988); (c) V. I. Fadeeva, T. I. Tikhomirova, I. B. Yuferova, G. V. Kudryavtsev. *Anal. Chim. Acta* **219**, 201 (1989).
153. (a) Yu. V. Kholin, I. V. Khristenko, D. S. Konyaev. *Russ. J. Phys. Chem.* **71**, 445 (1997); (b) Yu. V. Kholin, I. V. Khristenko. *Russ. J. Appl. Chem.* **70**, 897 (1997); (c) Y. V. Kholin, V. N. Zaitsev, E. Y. Gorlova, I. V. Khristenko. *Anal. Chim. Acta* **379**, 11 (1999).
154. (a) A. T. Pilipenko, O. S. Zulphikarov. *Hydroxamic Acids*, Nauka, Moscow (1989); (b) Y. K. Agrawal, S. G. J. Tandon. *Electroanal. Chem. Interfacial Electrochem.* **43**, 158 (1973); (c) M. T. Caudle, A. L. Crumbliss. *Inorg. Chem.* **33**, 4077 (1994); (d) B. Garcia, S. Ibeas, A. Munoz, J. M. Leal, C. Ghinami, F. Secco, M. Venturini. *Inorg. Chem.* **42**, 5434 (2003).
155. Yu. V. Kholin, V. N. Zaitsev, G. N. Zaitseva, L. S. Vasilik, S. A. Merny. *Russ. J. Inorg. Chem.* **40**, 261 (1995).
156. Yu. V. Kholin, S. A. Merny. *Zh. Fiz. Khim.* **69**, 1053 (1995).
157. Yu. V. Kholin, Yu. V. Shabaeva, I. V. Khristenko. *Russ. J. Appl. Chem.* **71**, 407 (1998).
158. V. N. Zaitsev, L. S. Vasilik, J. Evans, A. Brough. *Russ. Chem. Bull.* **48**, 2315 (1999).
159. V. N. Zaitsev, L. S. Kostenko, N. G. Kobylinskaya. *Anal. Chim. Acta* **565**, 157 (2006).
160. L. S. Kostenko, S. A. Akhmedov, V. N. Zaitsev. *Methods Objects Chem. Anal.* **1**, 116 (2006).
161. G. Anderegg, F. Arnaud-Neu, R. Delgado, J. Felcman, K. Popov. *Pure Appl. Chem.* **77**, 1445 (2005).
162. F. I. Belskii, I. B. Goryunova, P. V. Petrovskii, T. Y. Medved, M. I. Kabachnik. *Russ. Chem. Bull.* **31**, 93 (1982).

163. N. M. Dyatlova, V. Ya. Temkina, K. I. Popov. *Complexones and Metal Complexonates*, Khimiya, Moscow (1988).
164. E. I. Sinyavskaya. *Koord. Khim.* **18**, 899 (1992).